Crop rotational diversity alters the composition of stabilized soil organic matter compounds in soil physical fractions

Authors: Tong, Huan, Man, Meiling, Wagner-Riddle, Claudia, Dunfield, Kari E., Deen, Bill, et al.

Source: Canadian Journal of Soil Science, 103(1) : 213-233

Published By: Canadian Science Publishing

URL: https://doi.org/10.1139/cjss-2022-0058

Canadian Journal of Soil Science

Article

Crop rotational diversity alters the composition of stabilized soil organic matter compounds in soil physical fractions

Huan Tong[a], Meiling Man[a], Claudia Wagner-Riddle[b], Kari E. Dunfield[b], Bill Deen[c], and Myrna J. Simpson[a]

[a]Environmental NMR Centre and Department of Physical and Environmental Sciences, University of Toronto Scarborough, Toronto, ON M1C 1A4, Canada; [b]School of Environmental Sciences, University of Guelph, Guelph, ON N1G 2W1, Canada; [c]Department of Plant Agriculture, University of Guelph, Guelph, ON N1G 2W1, Canada

Corresponding author: **Myrna J. Simpson** (email: myrna.simpson@utoronto.ca)

Abstract

Crop rotational diversity is an important part of sustainable agricultural and soil management to improve crop yield and soil fertility including enhancing soil organic matter (SOM) stabilization. Because of the physical protection via interactions with soil minerals, SOM in mineral-associated fractions is believed to be longer-lived and more stable relative to SOM in particulate (light) fractions. However, it is still unclear how crop rotational diversity alters soil carbon distribution, composition and stabilization in soil physical fractions. To address this, we studied a 37 years' agricultural site with different crop rotational diversity (from continuous corn or alfalfa up to four species (corn, soybean, winter wheat, and red clover)). Soil carbon analysis, targeted compound analysis and nuclear magnetic resonance spectroscopy methods were used to obtain the distribution and degradation of SOM components in light and mineral-associated ($F_{53–2000\ \mu m}$, $F_{2–53\ \mu m}$, and $F_{<2\ \mu m}$) fractions. Higher soil organic carbon (SOC) concentrations were observed in $F_{<2\ \mu m}$ with relatively high diversified crop rotations (three and four types of crops) compared to monoculture or two crops in the rotations, which suggests that carbon storage is enhanced in mineral-stabilized pools. Higher concentrations of long-chain aliphatic compounds as well as increased accumulation and preservation of lignin-derived compounds in fine aggregates (<53 μm) were also observed with relatively high diversified crop rotations. Overall, the increased concentration and preservation of specific SOM compounds as well as increased SOC in finer mineral-associated fractions (<53 μm) suggests that crop rotational diversity may enhance the long-term stability of SOM in agroecosystems.

Key words: cutin, suberin, lignin, soil carbon concentration, nuclear magnetic resonance

Introduction

It is well established that soil organic matter (SOM) is critical for the stabilization of soil structure and maintenance of soil health and fertility (Soman et al. 2017; Srivastava et al. 2019; Yang et al. 2019). Continuously cropping with monoculture can lower soil organic carbon (SOC) concentration and soil fertility, thus decreasing plant productivity (Paustian et al. 2000; Lal 2004; Ren et al. 2018). In contrast, diversified crop rotations may maintain soil fertility and enhance crop yields (Reeves 1997; Gagnon et al. 2019; Agomoh et al. 2021; Janovicek et al. 2021). Some studies reported that high crop rotational diversity can build SOC via increased crop productivity and litter inputs to soil (West and Post 2002; Ogle et al. 2003; Hermle et al. 2008; Bai et al. 2018; Maiga et al. 2019). There is growing evidence that SOC in light fractions is less protected and more accessible for biodegradation (Six et al. 2002; Tonon et al. 2010; Poeplau et al. 2018; Haddix et al. 2020). In contrast, SOC in mineral-associated fractions is longer lived in the soil due to reduced availability for microbial decomposition (Jastrow et al. 2007; Sollins et al. 2009; Angst et al. 2017, 2018). Studies have also reported that diversified crop rotations may (Garcia et al. 2013; Moreira et al. 2018) or may not (Zotarelli et al. 2007) enhance SOC concentrations in light fractions in the short-term (<10 years). However, the SOC concentrations in light fractions were consistently increased in the long-term (>10 years) (Garcia et al. 2013; Li et al. 2018; Poffenbarger et al. 2020). In contrast, SOC stabilized in mineral-associated fractions reflected varied results after long-term diversified crop rotations (Freixo et al. 2002; Soon et al. 2007; Li et al. 2018; Moreira et al. 2018; Poffenbarger et al. 2020; Zhang et al. 2020). For example, some studies reported enhanced SOC concentrations in stabilized carbon pools (Li et al. 2018; Zhang et al. 2020), but others did not observe significant changes with long-term crop rotational diversity (Freixo et al. 2002; Poffenbarger et al. 2020). Therefore, applying diversified crop rotations to enhance SOC stability in a long-term manner still needs to be

further explored to better understand the benefits to agroecosystems.

High crop rotational diversity has also been reported to alter SOM molecular biogeochemical dynamics and stability (Lehmann et al. 2020; Savarese et al. 2021; Audette et al. 2021). For example, diversified crop litter inputs may stimulate microbial diversity and population, which subsequently altered SOM composition and stability (Lange et al. 2015; Audette et al. 2021). The distribution of SOM constituents may also be altered with varied compositional inputs of crop species. For example, leguminous biomass contributes more *O*-alkyl containing groups but less aromatics (Arshad et al. 2011); corn contributes less aliphatic lipids (Savarese et al. 2021); and wheat contributes more root-derived inputs (Agomoh et al. 2021). Also, high crop rotational diversity was found to shift SOM composition toward more long-lived components, such as aromatic carbons and aliphatic lipids (Zhao et al. 2021; Audette et al. 2021), and exhibited more preserved SOM in the long-term (>10 years) (Savarese et al. 2021; Audette et al. 2021). Some of the slowly decomposed compounds, namely long-chain aliphatic lipids, have been reported to accumulate in finer fractions via interactions with soil minerals, which were protected against microbial decomposition (Baldock et al. 1992; Guggenberger et al. 1995; Six et al. 2002; Helfrich et al. 2006; Tonon et al. 2010; Clemente et al. 2011; Saidy et al. 2013; Angst et al. 2017). Angeletti et al. (2021) measured SOM composition via solid-state ^{13}C nuclear magnetic resonance (NMR) spectroscopy and observed lower SOM decomposition states (alkyl/*O*-alkyl carbon) in mineral-associated aggregates with diversified crop rotations. This suggests that there may be significant benefits to using this management practice. However, more information is required to better understand how long-term crop rotational diversity alters SOM composition in different soil fractions.

Our previous study, which focused on analyzing whole soil samples from the same site, found changes in the distribution and degradation of SOM constituents with long-term crop rotational diversity despite minor differences in SOC concentrations (Man et al. 2021). This study highlighted the importance of molecular-level assessment of SOM biogeochemistry with land management practice (Man et al. 2021). For instance, higher concentrations of long-chain aliphatic lipids (*n*-alkanoic acids, *n*-alkanols, and hydrolyzable aliphatic lipids derived from cutin and suberin) were observed after long-term crop rotations with relatively high diversification (contained three or four types of crops) compared to low diversification and crop monoculture (Man et al. 2021). However, it is documented that carbon dynamics and biogeochemical cycling in light and mineral-associated SOM fractions are important for soil carbon stabilization (Guggenberger et al. 1995; Tonon et al. 2010; Clemente et al. 2011; Saidy et al. 2013; Lajtha et al. 2014; Angst et al. 2017; Angeletti et al. 2021), but this has not been explored in detail with the diversified crop rotations. The hypotheses of this study are that: (*i*) long-term highly diversified crop rotations increase the SOC concentrations in both light and mineral-associated fractions and (*ii*) highly diversified crop rotations accumulate more slowly decomposed components (e.g., long-chain aliphatic components) in mineral-associated fractions due to the organo-mineral interaction. The objective of this study is to assess the long-term effect of diversified crop rotation on the distribution and stabilization of SOM in fractions. To achieve this objective and test these hypotheses, soil samples from six different crop rotations from a 37 years' agriculture site at the Elora Research Station (Ontario, Canada) were fractionated and analyzed using elemental analysis and advanced molecular SOM characterization methods.

Materials and methods

Soil sampling, fractionation and carbon and nitrogen content analysis

Soil samples (0–10 cm) were collected from a long-term crop rotation experiment established in 1980 at the Elora research station, Ontario, Canada (Congreves et al. 2015). The soil at Elora was silty loam soil (Congreves et al. 2015). Samples were collected from six different crop rotations of 4 years' duration each, including continuous alfalfa ((*Medicago sativa* L.), AAAA), continuous corn ((*Zea mays* L.), CCCC), corn–corn–alfalfa–alfalfa (CCAA), corn–corn–soybean–soybean ((*Glycine max* (L.) Merr.), CCSS), corn–corn–soybean–winter wheat ((*Triticum aestivum* L.), CCSW), and corn–corn–soybean–winter wheat with red clover ((*Trifolium pretense* L.), $CCSW_{RC}$), under conventional tillage. Soil samples were collected before the harvest in October 2017. It was the second year of corn or alfalfa planting in the 4-year duration. The average tissue quality of carbon inputs and estimated SOC stabilization efficiency (by the ratio of SOC stock to total carbon inputs) of each crop rotation has been published in King et al. (2020). The collected soil samples were freeze-dried and passed through a 2 mm sieve. Then, soil samples from the same crop rotation treatment were combined from four field replicates as described in Man et al. (2021) before fractionation. Four different soil fractions were separated based on the density and the aggregate sizes. Briefly, approximately 250 g of sample was mixed with 500 mL 1.7 g/mL sodium iodide solution and mixed for 24 h. The mixture was centrifuged at 1500 rpm for 50 min (Clemente et al. 2011), the supernatant was collected and filtered using a GF/F glass microfiber filter (0.7 μm cut off; Whatman, Kent, UK), and then rinsed with deionized (18 MΩ cm at 25 °C) water. This step isolated the light fraction which was then transferred into tubes and freeze-dried for further analyses. The soil was not physically disrupted before further fractionation to preserve aggregate association, which are more representative of the biogeochemical function of SOM (Sollins et al. 2009). The residual heavy fraction was passed through a 53 μm sieve with deionized water. The soil aggregate fraction which was retained on the sieve was collected ($F_{53–2000\ \mu m}$). The fraction that passed through the sieve was then separated to two additional aggregate sizes ($F_{2–53\ \mu m}$ and $F_{<2\ \mu m}$) based on Stokes' law and sedimentation rates. The suspended portion ($F_{<2\ \mu m}$) was collected by aspiration and mixed with a 0.5 M calcium chloride solution to promote flocculation and avoid the loss of ultrafine particles. Deionized water was then used to rinse excess calcium chloride solution. All fractions were freeze-dried,

ground and stored at room temperature for further analyses. Soil carbon and nitrogen concentrations of each fractionated sample were analyzed using a Thermo Flash 2000 Elemental Analyzer (Thermo Scientific, Hudson, NH, USA). Samples were combusted at 950 °C under a stream of oxygen gas. The concentration of SOC and nitrogen was reported as an average of duplicate analyses.

Solid-state ^{13}C nuclear magnetic resonance (NMR) spectroscopy sample preparation and analysis

Three soil aggregate size fractions ($F_{53–2000\ \mu m}$, $F_{2–53\ \mu m}$ and $F_{<2\ \mu m}$) were repeatedly extracted with hydrofluoric acid (HF acid; 10% by volume in deionized water) to concentrate organic matter and decrease the concentration of paramagnetic materials which improves the signal to noise ratio in solid-state ^{13}C NMR analysis (Schmidt et al. 1997; Mitchell et al. 2018). Samples were rinsed with deionized water after HF treatment to remove excess salts and freeze-dried. Light fraction samples were not HF treated due to the low yield and high SOC concentration, which did not require pretreatment before NMR analyses. Samples were packed into a 4 mm zirconium rotor with a Kel-F cap and then characterized by solid-state ^{13}C cross-polarization magic angle spinning (CP-MAS) NMR spectroscopy. The NMR spectra were acquired using a 500 MHz Bruker BioSpin Avance III spectrometer (Bruker BioSpin, Rheinstetten, Germany) equipped with a 4 mm H–X MAS probe, using an 11 kHz spinning speed, a ramp-CP contact time of 1 ms, a recycle delay of 2 s with 40 960 scans for light fractions and $F_{<2\ \mu m}$ and a recycle delay of 1 s with 61 440 scans for $F_{53–2000\ \mu m}$ and $F_{2–53\ \mu m}$. Spectra were processed using a line broadening of 150 Hz. Four main chemical shift regions were used for the integration of ^{13}C NMR spectra and normalized to the total signal using Analysis of Mixtures (AMIX; v. 3.9.15) software (Bruker BioSpin, Rheinstetten, Germany): (*i*) alkyl carbon (0–50 ppm; from cutin, suberin, aliphatic side chains and lipids); (*ii*) *O*-alkyl carbon (50-110 ppm; from carbohydrates, peptides and methoxyl carbon in lignin); (*iii*) aromatic and phenolic carbon (110–165 ppm; from lignin and amino acids observed in peptides and black carbon) and (*iv*) carboxyl and carbonyl carbon (165–220 ppm; from fatty acids and amino acids in peptides and other degradation products) (Baldock et al. 1992; Preston et al. 1997; Simpson et al. 2008). The ratio of alkyl/*O*-alkyl carbon was calculated by dividing the integrated regions of alkyl carbon and *O*-alkyl carbon to establish the relative degradation stage of SOM in each fraction (Baldock et al. 1992; Baldock and Preston 1995; Preston et al. 1997; Kögel-Knabner 1997; Simpson and Simpson 2012).

Targeted soil organic matter (SOM) compounds extraction and analysis with gas chromatography – mass spectrometry (GC–MS)

Targeted SOM compounds with various microbial- and plant-derived sources were isolated and quantified using gas chromatography – mass spectrometry (GC–MS). Soil fractions were sequentially extracted in duplicate using solvent (dichloromethane/methanol), base hydrolysis and copper (II) oxide (CuO) oxidation extractions, which are described in detail in the Appendix A (Otto and Simpson 2005, 2006a, 2006b). The isolated compounds (including aliphatic lipids, steroids, as well as the cutin-, suberin-, and lignin-derived compounds) from each extraction step were analyzed by GC–MS using established methods (Otto and Simpson 2005, 2006a, 2006b). Briefly, soil fractions (light fraction 0.2 g; $F_{53–2000\ \mu m}$ and $F_{2–53\ \mu m}$ 15 g and $F_{<2\ \mu m}$ 3 g) were solvent-extracted sequentially with dichloromethane, dichloromethane and methanol mixture (1:1 by volume), and methanol to isolate the solvent-extractable SOM components in each fraction (Otto and Simpson 2005). Air-dried solvent extracted samples were then base hydrolyzed with methanolic potassium hydroxide (KOH, 1 M in methanol) solution in Teflon lined bombs at 100 °C for 3 h to obtain ester-bound lipids (Goñi and Hedges 1990b; Otto and Simpson 2006a). The base hydrolyzed samples were then oxidized with 1 g CuO, 100 mg ammonium iron (II) sulphate hexahydrate $[Fe(NH_4)_2(SO_4)_2{\cdot}6H_2O]$ and 15 mL of sodium hydroxide (NaOH, 2 M in deionized water) in Teflon lined bombs at 170 °C for 2.5 h (Hedges and Ertel 1982; Hedges et al. 1988; Otto and Simpson 2006b). Then the supernatants were solid-phase extracted using HLB SPE cartridges (Waters Limited, Mississauga, ON, Canada) to obtain the lignin-derived compounds (Pinto et al. 2010).

All the soil extracts were derivatized before GC–MS analysis so that the targeted compounds are more volatile and amenable to GC separation and analysis (Otto and Simpson 2005, 2006a, 2006b). Compounds isolated via solvent and CuO oxidation extraction were derivatized using *N, O*-bis(trimethylsilyl)trifluoroacetamide and pyridine. Base hydrolysis extraction products were first methylated using *N, N*-dimethylformamide dimethyl acetal and then derivatized with *N, O*-bis(trimethylsilyl)trifluoroacetamide and pyridine. The derivatized samples were analyzed by GC–MS using an Agilent 7890B gas chromatograph equipped with a 5977B mass spectrometer operated with electron impact (70 eV) ionization. Samples were diluted with hexane and 1 μL of each sample was injected using an Agilent 7603 A automatic sampler at an inlet temperature of 280 °C onto an HP-5MS fused silica capillary column (30 m × 0.25 mm i.d. × 0.25 μm film thickness). The oven temperature gradient started at 65 °C for 2 min, followed by an increase of 6 °C min^{-1} to 300 °C, and then a 20 min isothermal hold. The flow rate of carrier gas (helium) was 1 mL min^{-1}. Data acquisition was performed using Agilent Mass Hunter GC–MS Acquisition (version B.07.03.2129) and data were processed using Agilent Enhanced ChemStation software (version E.02.02.1431). The identification of the targeted compounds was obtained by comparing the mass spectra with Wiley Registry (9th edition) plus the National Institute of Standards and Technology (NIST) mass spectral databases, the mass spectral library of soil compounds and published mass spectra. External standards were used to quantify the concentration of targeted compounds from extractions (Otto and Simpson 2005, 2006a, 2006b). Tetracosane, 1-docosanol, methyl tricosanoate and cholesterol were used as external standards for solvent extractable compounds. Methyl tricosanoate was used as an external standard for cutin- and suberin-derived compounds,

and vanillic acid and vanillin were used as external standards for lignin-derived phenols.

Solvent extractable compounds included: short-chain aliphatic lipids ($<C_{20}$, *n*-alkanes, *n*-alkanols, and *n*-alkanoic acids), long-chain aliphatic lipids ($\geq C_{20}$, *n*-alkanes, *n*-alkanols, and *n*-alkanoic acids), and cyclic lipids (cholesterol, ergosterol, campesterol, stigmasterol, sitosterol and stigmastanol) (Otto and Simpson 2005). Cutin-derived compound concentrations (ΣC) were calculated as the sum of mid-chain hydroxy C_{14}, C_{15}, C_{17} acids, C_{16} mono- and dihydroxy acids and diacids (Otto and Simpson 2006a). The *ω*-hydroxy C_{16} acids (*ω*-C_{16}) are relatively more persistent than other fatty acids, thus the increased abundance of *ω*-C_{16} in C_{16} hydroxy acids (*ω*-C_{16}/ΣC_{16}) is indicative of cutin decomposition (Otto and Simpson 2006a). The concentration of suberin-derived compounds (ΣS) was calculated as the sum of long-chain *ω*-hydroxyalkanoic acids (C_{20}–C_{32}), *α*,*ω*-diacids (C_{20}–C_{32}) and 9,10-epoxy-18-hydroxy C_{18} dioic acid (Otto and Simpson 2006a). Suberin- or cutin-derived compounds concentration (ΣSvC) was calculated as the sum of *ω*-hydroxyalkanoic acids C_{16}, C_{18}, C_{18} di- and trihydroxy acids, 9,10-epoxy-*ω*-hydroxy C_{18} acid, and *α*, *ω*-diacids C_{16}, C_{18} (Otto and Simpson 2006a). The ratio of suberin- to cutin-derived compounds (suberin/cutin ratio, which was calculated as (ΣS+ΣSvC)/(ΣC+ΣSvC)) informs root-derived (ratio > 1) or leave-derived (ratio < 1) sources (Otto and Simpson 2006a). The concentrations of lignin-derived phenols were calculated as the sum of cinnamyl (*p*-coumaric acid and ferulic acid), syringyl (syringic acid, syringaldehyde and acetosyringone), and vanillyl (vanillic acid, vanillin and acetovanillone) phenols (Goñi and Hedges 1990a; Otto and Simpson 2006b). Ratios of syringyl to vanillyl (syringyl/vanillyl) phenols versus the ratios of cinnamyl to vanillyl (cinnamyl/vanillyl) phenols can discriminate different lignin sources (Hedges and Ertel 1982; Hedges et al. 1988; Goñi and Hedges 1990a; Otto and Simpson 2006b). The oxidation state of lignin was determined by the acid to aldehyde ratios of two lignin monomer classes, vanillyl ($(Ad/Al)_v$) and syringyl ($(Ad/Al)_s$), which increase with progressive degradation (Hedges et al. 1988).

Statistical analyses

Statistical analyses were performed using IBM SPSS Statistics version 22. Independent samples *t*-test was used to examine the differences in soil chemical properties (i.e., soil carbon and nitrogen contents as well as concentration and degradation of groups of SOM components) between crop rotations in each soil fraction with a significant level of $P < 0.05$ and $n = 2$. The independent samples *t*-test analysis was also used to examine the significant differences ($P < 0.05$) of SOM characteristics (e.g., groups of SOM components concentration and degradation) between relatively low (AAAA, CCCC, CCAA, and CCSS, in total $n = 8$) and high (CCSW and $CCSW_{RC}$, in total $n = 4$) crop rotational diversity in each soil fraction. Linear regression was used to evaluate the relationships of the SOM characteristics between whole soil and fractionated samples (including SOC concentration, carbon to nitrogen (C: N) ratio, the relative contribution of different functional groups and alkyl/*O*-alkyl carbon ratio from ^{13}C NMR spectroscopy, targeted compounds concentration and the degradation proxies for specific groups).

Results

Soil carbon and nitrogen analysis

The mass recovery of samples from different crop rotations was greater than 97% (Table A1). The carbon recovery of the samples ranged from 86% to 95% (Table A1). The SOC concentration was highest in the light fractions followed by the $F_{<2\ \mu m}$, $F_{53–2000\ \mu m}$ to $F_{2–53\ \mu m}$ fractions (Table 1). Higher SOC concentrations were observed in light and $F_{<2\ \mu m}$ fractions compared to whole soil (Table 1). Within the same soil fraction, SOC concentrations from different crop rotations exhibited significant differences ($P < 0.05$, Table 1). For example, the SOC concentrations in light fractions were significantly different between crop rotations (Table 1). Within the same mineral fraction ($F_{53–2000\ \mu m}$, $F_{2–53\ \mu m}$ or $F_{<2\ \mu m}$), there were fewer significant differences observed between rotations compared to the light fractions. The SOC concentrations in mineral fractions ($F_{53–2000\ \mu m}$, $F_{2–53\ \mu m}$ and $F_{<2\ \mu m}$) with the AAAA treatment were the highest compared to other crop rotations (Table 1). Significant differences were observed in SOC concentrations in light fractions and $F_{2–53\ \mu m}$ between relatively high and low crop rotational diversities (Table 2). Higher SOC concentrations were observed in light fractions from relatively high diversified crop rotations (CCSW and $CCSW_{RC}$) and in $F_{2–53\ \mu m}$ from low diversified crop rotations (AAAA, CCCC, CCAA and CCSS; Table 2). The C: N ratios decreased from light fractions, $F_{53–2000\ \mu m}$, $F_{2–53\ \mu m}$ to $F_{<2\ \mu m}$ among all crop rotations whereas the C: N ratio of the unfractionated soil samples was only higher than $F_{<2\ \mu m}$ ratios.

Solid-state ^{13}C nuclear magnetic resonance (NMR) analysis

The NMR spectra from all crop rotations exhibited similar chemical signatures (Fig. A1) but different abundances of SOM components (Table 3). Alkyl carbon was relatively higher in the $F_{<2\ \mu m}$ (29%–31%) than in other fractions analyzed (Table 3). The relative abundance of *O*-alkyl carbon were observed to be higher in $F_{53–2000\ \mu m}$ (45%–46%) and $F_{2–53\ \mu m}$ (42%–43%) than in $F_{<2\ \mu m}$ (27%–32%). The highest relative contribution of aromatic and phenolic carbon was observed in light fractions (20%–30%) and the lowest relative contribution was found in $F_{<2\ \mu m}$ (16%–18%). The highest relative abundance of carboxylic and carbonyl carbon was in $F_{<2\ \mu m}$ (22%–26%) and lowest was in $F_{53–2000\ \mu m}$ (8%–9%) across crop rotations. The relative degradation state of SOM (alkyl/*O*-alkyl carbon), which increases with progressive organic matter degradation (Baldock et al. 1992; Preston et al. 1997; Kögel-Knabner 1997), was higher from $F_{53–2000\ \mu m}$, $F_{2–53\ \mu m}$ to $F_{<2\ \mu m}$. The light fraction had the lowest alkyl/*O*-alkyl carbon ratio compared to mineral-bound fractions. The alkyl/*O*-alkyl carbon ratio of $F_{<2\ \mu m}$ was closer to the ratio of the whole soil than other fractions (Table 3).

Within the same fraction class, similar trends of the relative contribution of groups of SOM were observed, except for light fractions and $F_{<2\ \mu m}$ with monoculture crops (AAAA

Table 1. Soil organic carbon (SOC) concentration (with the unit g OC/kg soil for whole soil and g OC/kg fraction for soil fractions) and carbon to nitrogen (C: N) ratios (standard error from duplicate samples) of $F_{53–2000\ \mu m}$, $F_{2–53\ \mu m}$, $F_{<2\ \mu m}$, and light fraction was compared to whole soil (Man et al. 2021).

	Whole soil	Light fraction	$F_{53–2000\ \mu m}$	$F_{2–53\ \mu m}$	$F_{<2\ \mu m}$
SOC concentration					
AAAA	25.9	281.4 ± 1.9b	20.6 ± 0.5a	16.1 ± 0.2a	64.7 ± 1.2a,b
CCCC	22.6	245.1 ± 0.2d	16.2 ± 0.7b	10.5 ± 0.3c	57.2 ± 1.3b,c
CCAA	23.8	259.5 ± 1.7c	19.2 ± 0.9a,b	10.8 ± 0.2b,c	56.0 ± 0.6c
CCSS	19.5	180.9 ± 0.3e	17.3 ± 0.6a,b	9.3 ± 0.9b,d	51.2 ± 2.1c
CCSW	21.2	295.3 ± 0.3a	14.7 ± 0.9b	9.0 ± 0.1d	56.1 ± 1.0c
$CCSW_{RC}$	21.8	283.7 ± 1.0b	19.1 ± 0.3a	8.8 ± 0.3c,d	61.3 ± 0.4b
C: N ratio					
AAAA	9.63	15.3 ± 0.1d	13.1 ± 0.1c	12.0 ± 0.1b,c	7.7 ± 0.2a,b,c
CCCC	10.25	19.5 ± 0.2a	16.8 ± 0.1a	11.9 ± 0.1c	8.2 ± 0.0a
CCAA	9.94	17.3 ± 0.2b,c	15.3 ± 0.1b	11.6 ± 0.1c,d	7.5 ± 0.0c
CCSS	10.05	18.7 ± 0.0b	18.3 ± 1.0a,b	13.0 ± 0.1a	7.9 ± 0.1a,b,c
CCSW	9.95	19.7 ± 0.6a,b,c	16.7 ± 0.8a,b	11.3 ± 0.1a,d	7.6 ± 0.1b,c
$CCSW_{RC}$	9.65	18.1 ± 0.1c	16.8 ± 0.4a,b	12.3 ± 0.0b	7.9 ± 0.0b

Note: AAAA, CCCC, CCAA, CCSS, CCSW and $CCSW_{RC}$ represent continuous alfalfa, continuous corn, corn–corn–alfalfa–alfalfa, corn–corn–soybean–soybean, corn–corn–soybean–winter wheat, and corn–corn–soybean–winter wheat with red clover, respectively. SOC concentration or C: N ratio of samples is significantly different from other crop rotations within the same soil fraction at $P < 0.05$; significant differences between crop rotations are represented by different letters.

and CCCC). In diversified crop rotations, the relative contribution of SOM components from light fraction samples decreased from *O*-alkyl carbon, aromatic and phenolic carbon, alkyl carbon to carboxyl and carbonyl carbon (Table 3). The AAAA light fraction had relatively higher alkyl carbon (23%) than aromatic and phenolic carbon (20%), and the CCCC had slightly higher carboxyl and carbonyl carbon (17%) than alkyl carbon (16%). In $F_{<2\ \mu m}$, the relative contribution of components from high to low was alkyl carbon, *O*-alkyl carbon, carboxyl and carbonyl carbon and aromatic and phenolic carbon for samples from diversified crop rotations (Table 3). AAAA and CCCC had relatively higher *O*-alkyl carbon (32%) than alkyl carbon (29%–30%) in the $F_{<2\ \mu m}$.

Targeted soil organic matter (SOM) compounds analysis by gas chromatography – mass spectrometry (GC–MS)

The concentration of solvent extractable compounds (*n*-alkanes, *n*-alkanols, *n*-alkanoic acids and steroids) differed among soil fractions (Fig. 1). Higher concentrations of plant-derived steroids and *n*-alkanoic acids were observed in light fractions and $F_{53–2000\ \mu m}$ in comparison to $F_{2–53\ \mu m}$ and $F_{<2\ \mu m}$. The concentrations of *n*-alkanoic acids and plant-derived steroids in light fractions were much higher than in the unfractionated soil (Fig. 1). In contrast, *n*-alkane and *n*-alkanol concentrations were higher in $F_{2–53\ \mu m}$ and $F_{<2\ \mu m}$ than in light fraction and $F_{53–2000\ \mu m}$ for all crop rotations (Fig. 1). $F_{<2\ \mu m}$ contained a much higher concentration of *n*-alkanols than the whole soil (Fig. 1). The concentrations of long-chain *n*-alkanes and *n*-alkanols ($\geq C_{20}$) in $F_{53–2000\ \mu m}$ and soil samples were inversely correlated (Fig. A2). Positive linear correlations were observed between concentrations of long-chain *n*-alkanes and *n*-alkanols ($\geq C_{20}$) in $F_{2–53\ \mu m}$ and whole soils across crop rotations (Fig. A2). *N*-alkanes, *n*-alkanols and steroids from all fractionated samples were predominantly plant-derived ($\geq C_{20}$, Fig. 1 and Table A2). For the light fractions, $F_{53–2000\ \mu m}$ and $F_{2–53\ \mu m}$, the main contribution of *n*-alkanoic acids are microbial-derived compounds ($< C_{20}$, Fig. 1 and Table A2) for all crop rotations.

Within the same fraction class, a few solvent extractable compound concentrations in relatively high diversified (more than two crop species) crop rotations were significantly different compared to low diversified (monoculture or two crop species) crop rotations ($P < 0.05$, Table 2). In light fractions, concentrations of long-chain aliphatic lipids, *n*-alkanes, and *n*-alkanols in highly diversified crop rotations (CCSW and $CCSW_{RC}$) were significantly lower than in low diversified crop rotations (AAAA, CCCC, CCAA, and CCSS; $P < 0.05$, Table 2). The plant-derived steroids and cyclic lipids concentrations in relatively high diversified crop rotations (CCSW and $CCSW_{RC}$) were higher than the concentrations in low diversified crop rotations (AAAA, CCCC, CCAA, and CCSS) in $F_{53–2000\ \mu m}$ and $F_{2–53\ \mu m}$ (Table 2). AAAA exhibited the most distinctive results compared to other crop rotations within the same fraction class or in soil samples (Fig. 1). For example, AAAA exhibited higher concentrations of long-chain aliphatic lipids ($\geq C_{20}$) in the light fraction and $F_{53–2000\ \mu m}$ than other crop rotations (Table A2). Significantly higher concentrations of total *n*-alkane and long-chain *n*-alkanes ($\geq C_{20}$) of AAAA in $F_{53–2000\ \mu m}$ ($P < 0.05$) but lower in $F_{2–53\ \mu m}$ or $F_{<2\ \mu m}$ than in other crop rotations were observed (Table A2). The concentration of short-chain *n*-alkanols ($< C_{20}$) of AAAA in the light fraction was higher than other crop rotations ($P < 0.05$, Table A2), and long-chain *n*-alkanols ($\geq C_{20}$) and total *n*-alkanols concentrations of AAAA in $F_{53–2000\ \mu m}$ were higher than other crop rotations ($P < 0.05$, Table A2).

Higher concentrations of cutin- and suberin-derived compounds were observed in $F_{<2\ \mu m}$ than in other fractions or whole soil among different crop rotations (Figs. 2*a* and 2*b*).

Table 2. Soil organic carbon (SOC) concentration, carbon to nitrogen ratio, the relative contribution of alkyl, *O*-alkyl, aromatic and phenolic and carboxyl and carbonyl carbon, alkyl/*O*-alkyl carbon ratio, and specific groups of compounds (solvent extractable compounds, cutin- and/or suberin-derived compounds, and lignin-derived phenols) concentrations (which were normalized to SOC concentration of fractions, μg/g OC) and degradation between relatively low (AAAA, CCCC, CCAA and CCSS; mean ± standard error) and high diversified (CCSW and $CCSW_{RC}$; mean ± standard error) crop rotations.

	Light fraction		$F_{53-2000\ \mu m}$ fraction		$F_{2-53\ \mu m}$ fraction		$F_{<2\ \mu m}$ fraction	
	Low diversity	High diversity	Low diversity	High diversity	Low diversity	High diversity	Low diversity	High diversity
SOC concentration (g OC/kg fraction)	**241.7 ± 14.2**	**289.5 ± 3.4**	18.3 ± 0.7	16.9 ± 1.3	**11.7 ± 1.0**	**8.9 ± 0.1**	57.2 ± 1.9	58.7 ± 1.6
Carbon to nitrogen ratio	17.7 ± 0.6	18.9 ± 0.5	15.9 ± 0.8	16.7 ± 0.4	12.1 ± 0.2	11.8 ± 0.3	7.8 ± 0.1	7.7 ± 0.1
Alkyl carbon (%)	19.3 ± 1.5	17.5 ± 1.5	25.0 ± 0.4	23.5 ± 0.5	26.8 ± 0.5	26.0 ± 0.0	29.8 ± 0.5	29.5 ± 0.5
O-alkyl carbon (%)	40.0 ± 1.1	40.5 ± 0.5	45.3 ± 0.3	45.0 ± 0.0	42.5 ± 0.3	42.5 ± 0.5	29.8 ± 1.3	28.0 ± 0.0
Aromatic and phenolic carbon (%)	26.3 ± 2.2	27.5 ± 1.5	21.0 ± 0.7	23.0 ± 0.0	21.3 ± 0.5	22.0 ± 0.0	16.5 ± 0.5	18.0 ± 0.0
Carboxyl and carbonyl carbon (%)	14.5 ± 0.9	14.5 ± 0.5	8.8 ± 0.3	8.5 ± 0.5	9.5 ± 0.3	9.5 ± 0.5	24.0 ± 0.9	24.5 ± 0.5
Alkyl/*O*-alkyl carbon ratio	0.5 ± 0.0	0.4 ± 0.0	0.6 ± 0.0	0.5 ± 0.0	0.6 ± 0.0	0.6 ± 0.0	1.0 ± 0.1	1.0 ± 0.0
Short-chain *n*-alkanes ($<C_{20}$)	**11.8 ± 1.2**	**15.4 ± 0.3**	9.2 ± 1.1	6.3 ± 2.8	3.5 ± 0.8	3.8 ± 1.9	10.6 ± 1.7	8.5 ± 1.6
Long-chain *n*-alkanes ($\geq C_{20}$)	**64.6 ± 5.5**	**44.2 ± 1.4**	170.8 ± 24.7	126.7 ± 1.0	95.6 ± 9.5	113.5 ± 4.3	169.8 ± 6.4	168.8 ± 6.2
Total *n*-alkanes	**76.3 ± 6.3**	**59.6 ± 1.5**	180.0 ± 25.5	133.0 ± 3.8	99.1 ± 9.7	117.3 ± 2.8	180.4 ± 5.7	177.3 ± 5.7
Short-chain *n*-alkanols ($<C_{20}$)	31.8 ± 5.0	26.1 ± 5.0	24.6 ± 2.9	26.8 ± 3.8	11.1 ± 1.0	15.4 ± 2.7	13.7 ± 1.3	16.0 ± 0.9
Long-chain *n*-alkanols ($\geq C_{20}$)	**224.5 ± 19.0**	**74.9 ± 1.1**	367.9 ± 46.2	313.2 ± 15.0	**390.5 ± 16.4**	**450.6 ± 13.3**	828.9 ± 34.1	806.2 ± 24.1
Total *n*-alkanols	**256.3 ± 23.7**	**101.0 ± 5.3**	392.5 ± 45.8	340.0 ± 18.6	**401.6 ± 17.0**	**466.0 ± 14.8**	842.6 ± 33.6	822.2 ± 23.9
Short-chain *n*-alkanoic acids ($<C_{20}$)	7375.3 ± 436.1	8062.3 ± 518.4	1594.7 ± 65.5	1821.3 ± 122.5	462.3 ± 62.4	572.1 ± 39.4	246.1 ± 7.5	310.1 ± 42.1
Long-chain *n*-alkanoic acids ($\geq C_{20}$)	495.4 ± 32.8	433.2 ± 22.4	487.2 ± 26.7	499.7 ± 61.7	289.1 ± 35.5	327.5 ± 16.1	260.6 ± 28.1	225.7 ± 31.6
Total *n*-alkanoic acids	7870.7 ± 439.3	8495.5 ± 504.5	2081.9 ± 81.5	2321.0 ± 183.9	751.3 ± 80.2	899.6 ± 53.0	506.8 ± 25.9	535.8 ± 73.0
Short-chain aliphatic lipids[a]	7418.8 ± 434.2	8103.8 ± 523.5	1628.5 ± 63.1	1854.4 ± 128.8	476.8 ± 63.1	591.3 ± 43.1	270.4 ± 7.9	334.6 ± 44.3
Long-chain aliphatic lipids[b]	**784.4 ± 47.6**	**552.4 ± 22.7**	1025.8 ± 86.1	939.6 ± 77.2	775.2 ± 53.4	891.6 ± 29.0	1259.4 ± 21.1	1200.7 ± 26.2
Fungal-derived steroid[c]	7.8 ± 0.4	7.7 ± 0.1	14.5 ± 4.8	23.3 ± 4.0	1.4 ± 0.3	9.8 ± 3.1	1.7 ± 0.3	1.9 ± 0.4
Plant-derived steroids[d]	734.1 ± 39.7	714.3 ± 14.4	**178.7 ± 4.5**	**207.5 ± 7.3**	**91.1 ± 6.1**	**144.3 ± 1.8**	132.9 ± 5.8	133.6 ± 4.1
Cyclic lipids[e]	804.0 ± 37.2	789.7 ± 13.3	**218.3 ± 6.6**	**269.5 ± 12.3**	**102.9 ± 6.6**	**171.7 ± 2.3**	157.9 ± 5.6	165.6 ± 7.8
Suberin-derived compounds[f]	188.9 ± 17.9	200.4 ± 10.9	175.2 ± 12.5	171.5 ± 4.8	253.5 ± 34.0	215.5 ± 10.8	2627.8 ± 248.6	3128.4 ± 108.6
Cutin-derived compounds[g]	70.6 ± 6.0	50.1 ± 8.7	215.1 ± 52.2	69.6 ± 3.9	230.7 ± 28.0	219.8 ± 12.8	5086.5 ± 601.6	4601.1 ± 334.2
Suberin- and cutin-derived compounds[h]	**1143.1 ± 138.0**	**761.0 ± 20.1**	**866.4 ± 110.5**	**523.2 ± 11.6**	893.5 ± 65.8	763.5 ± 13.5	11 303.5 ± 470.7	12 062.9 ± 438.2
ω-$C_{16}/\Sigma C_{16}$[i]	0.13 ± 0.01	0.13 ± 0.03	0.10 ± 0.02	0.10 ± 0.01	0.08 ± 0.01	0.08 ± 0.00	0.07 ± 0.00	0.07 ± 0.01
Lignin-derived phenols[j]	9245.2 ± 636.3	9952.3 ± 392.2	1829.5 ± 175.1	2009.4 ± 106.5	2945.9 ± 400.2	3237.8 ± 54.2	1348.3 ± 79.4	1216.0 ± 98.4
$(Ad/Al)_v$[k]	1.10 ± 0.06	1.13 ± 0.05	1.86 ± 0.07	1.80 ± 0.02	3.91 ± 1.66	2.26 ± 0.02	4.93 ± 0.44	3.70 ± 0.30
$(Ad/Al)_s$[l]	1.23 ± 0.06	1.20 ± 0.07	1.88 ± 0.05	1.97 ± 0.14	3.63 ± 1.64	2.22 ± 0.01	2.63 ± 0.34	2.75 ± 0.18

Note: AAAA, CCCC, CCAA, CCSS, CCSW and $CCSW_{RC}$ represent continuous alfalfa, continuous corn, corn–corn–alfalfa–alfalfa, corn–corn–soybean–soybean, corn–corn–soybean–winter wheat, and corn–corn–soybean–winter wheat with red clover, respectively. Significant levels at $P < 0.05$ after the *t*-test are in bold.

[a]Short-chain aliphatic lipids: sum of short-chain ($<C_{20}$) *n*-alkanes, *n*-alkanols and *n*-alkanoic acids.

[b]Long-chain aliphatic lipids: sum of long-chain ($\geq C_{20}$) *n*-alkanes, *n*-alkanols and *n*-alkanoic acids.

[c]Fungal-derived steroid: ergosterol (Otto and Simpson 2005).

[d]Plant-derived steroids: sum of campesterol, stigmasterol, sitosterol and stigmastanol (Otto and Simpson 2005).

[e]Cyclic lipids: sum of ergosterol, cholesterol, campesterol, stigmasterol, sitosterol and stigmastanol (Otto and Simpson 2005).

[f]Suberin-derived compounds: sum of suberin-derived compounds (ω-hydroxy acids C_{20}–C_{32}, α,ω-diacids C_{20}–C_{32}, and 9,10-ep C_{18} dioic acid) (Otto and Simpson 2006a).

[g]Cutin-derived compounds: sum of cutin-derived compounds (mid-chain hydroxy C_{14}, C_{15}, C_{17} acids, C_{16} mono- and dihydroxy acids and diacids) (Otto and Simpson 2006a).

[h]Suberin- and cutin-derived compounds: sum of suberin-derived compounds, cutin-derived compounds and suberin- or cutin-derived compounds (ω-hydroxyalkanoic acids C_{16}, C_{18}, C_{18} di- and trihydroxy acids, 9,10-epoxy-ω-hydroxy C_{18} acid, and α, ω-diacids C_{16}, C_{18} (Otto and Simpson 2006a)).

[i]ω-$C_{16}/\Sigma C_{16}$: cutin degradation state was calculated by the ratio of ω-hydroxy C_{16} acid to the sum of ω-hydroxy C_{16} acid, α,ω-dioic C_{16} acid and C_{16} mid-chain-substituted acids (Otto and Simpson 2006a).

[j]Lignin-derived phenols: sum of cinnamyls (*p*-coumaric acid and ferulic acid), syringyls (syringaldehyde, acetosyringone and syringic acid) and vanillyls (vanillin, acetovanillone and vanillic acid) (Otto and Simpson 2006b).

[k]$(Ad/Al)_v$: ratio of vanillic acid to vanillin (Goñi and Hedges 1990a; Otto and Simpson 2006b).

[l]$(Ad/Al)_s$: ratio of syringic acid to syringaldehyde (Goñi and Hedges 1990a; Otto and Simpson 2006b).

Table 3. Relative contribution (%) of alkyl (0–50 ppm), *O*-alkyl (50–110 ppm), aromatic and phenolic (110–165 ppm) and carboxyl and carbonyl (165–220 ppm) carbon (Baldock et al. 1992; Preston et al. 1997; Simpson et al. 2008) integrated from solid-state ^{13}C NMR spectra with the alkyl/*O*-alkyl carbon ratios (Baldock and Preston 1995; Preston et al. 1997; Kögel-Knabner 1997; Simpson and Simpson 2012) from whole soil (Man et al. 2021) and different soil fractions.

	Whole soil	Light fraction	$F_{53–2000\ \mu m}$	$F_{2–53\ \mu m}$	$F_{<2\ \mu m}$
Continuous alfalfa (AAAA)					
Alkyl (%)	25	23	26	28	29
O-alkyl (%)	25	43	46	42	32
Aromatic and phenolic (%)	31	20	19	20	16
Carboxyl and carbonyl (%)	19	14	9	10	23
Alkyl/*O*-alkyl	0.98	0.53	0.57	0.67	0.89
Continuous corn (CCCC)					
Alkyl (%)	28	16	24	27	30
O-alkyl (%)	26	40	45	43	32
Aromatic and phenolic (%)	29	27	22	21	16
Carboxyl and carbonyl (%)	17	17	9	9	22
Alkyl/*O*-alkyl	1.08	0.40	0.53	0.63	0.95
Corn–corn–alfalfa–alfalfa					
Alkyl (%)	24	20	25	26	29
O-alkyl (%)	27	39	45	43	27
Aromatic and phenolic (%)	30	28	21	22	18
Carboxyl and carbonyl (%)	19	13	9	9	26
Alkyl/*O*-alkyl	0.91	0.51	0.56	0.60	1.10
Corn–corn–soybean–soybean					
Alkyl (%)	32	18	25	26	31
O-alkyl (%)	22	38	45	42	28
Aromatic and phenolic (%)	28	30	22	22	16
Carboxyl and carbonyl (%)	18	14	8	10	25
Alkyl/*O*-alkyl	1.44	0.47	0.56	0.62	1.08
Corn–corn–soybean–winter wheat					
Alkyl (%)	31	16	23	26	29
O-alkyl (%)	23	40	45	42	28
Aromatic and phenolic (%)	28	29	23	22	18
Carboxyl and carbonyl (%)	18	15	9	10	25
Alkyl/*O*-alkyl	1.33	0.40	0.51	0.62	1.02
Corn–corn–soybean–winter wheat with red clover					
Alkyl (%)	30	19	24	26	30
O-alkyl (%)	23	41	45	43	28
Aromatic and phenolic (%)	29	26	23	22	18
Carboxyl and carbonyl (%)	18	14	8	9	24
Alkyl/*O*-alkyl	1.30	0.46	0.53	0.60	1.05

Positive correlations were observed between suberin-derived and suberin- and cutin-derived compounds concentrations in $F_{<2\ \mu m}$ and in whole soil (Fig. A2). Samples from $F_{<2\ \mu m}$ had a relatively lower cutin degradation state (ω-$C_{16}/\Sigma C_{16}$) compared to other fractions for the majority of crop rotations, but this fraction was more degraded than whole soil (Fig. 2*c*). The suberin/cutin ratios varied in fractions across crop rotations but were mostly lower than the ratios of soil (Fig. 2*d*). Lower concentrations of suberin- and cutin-derived compounds with significance ($P < 0.05$) were observed in relatively high diversified crop rotations (CCSW and CCSWRC) compared to low diversity (AAAA, CCCC, CCAA and CCSS) only in the light fractions and $F_{53–2000\ \mu m}$ (Table 2). The concentrations of suberin- and cutin-derived compounds also varied with crop species in the $F_{<2\ \mu m}$. Crops containing alfalfa (AAAA and CCAA) had relatively lower suberin-derived compounds and higher cutin-derived compounds than soybean-containing treatments (CCSS, CCSW and $CCSW_{RC}$; Table A3) in the $F_{<2\ \mu m}$.

Identified and quantified lignin-derived phenols (Table A4) included: cinnamyl (*p*-coumaric acid and ferulic acid, Fig. 3*a*), syringyl (syringic acid, syringaldehyde and acetosyringone, Fig. 3*b*), and vanillyl (vanillic acid, vanillin, acetovanillone, Fig. 3*c*) classes (Goñi and Hedges 1990a;

Fig. 1. The concentrations of solvent extractable compounds (*n*-alkanes, *n*-alkanols, *n*-alkanoic acids and steroids, which the concentrations were normalized to soil organic carbon content of whole soil or fractions) among different crop rotational diversity within the whole soil (Man et al. 2021), light fractions, $F_{53–2000\ \mu m}$, $F_{2–53\ \mu m}$ and $F_{<2\ \mu m}$ (error bars indicate the standard error, $n = 3$ for whole soil (Man et al. 2021) and $n = 2$ for fraction samples). The concentration ranges on the *y*-axis were different for each graph. AAAA, CCCC, CCAA, CCSS, CCSW, and $CCSW_{RC}$ represent continuous alfalfa, continuous corn, corn–corn–alfalfa–alfalfa, corn–corn–soybean–soybean, corn–corn–soybean–winter wheat, and corn–corn–soybean–winter wheat with red clover, respectively.

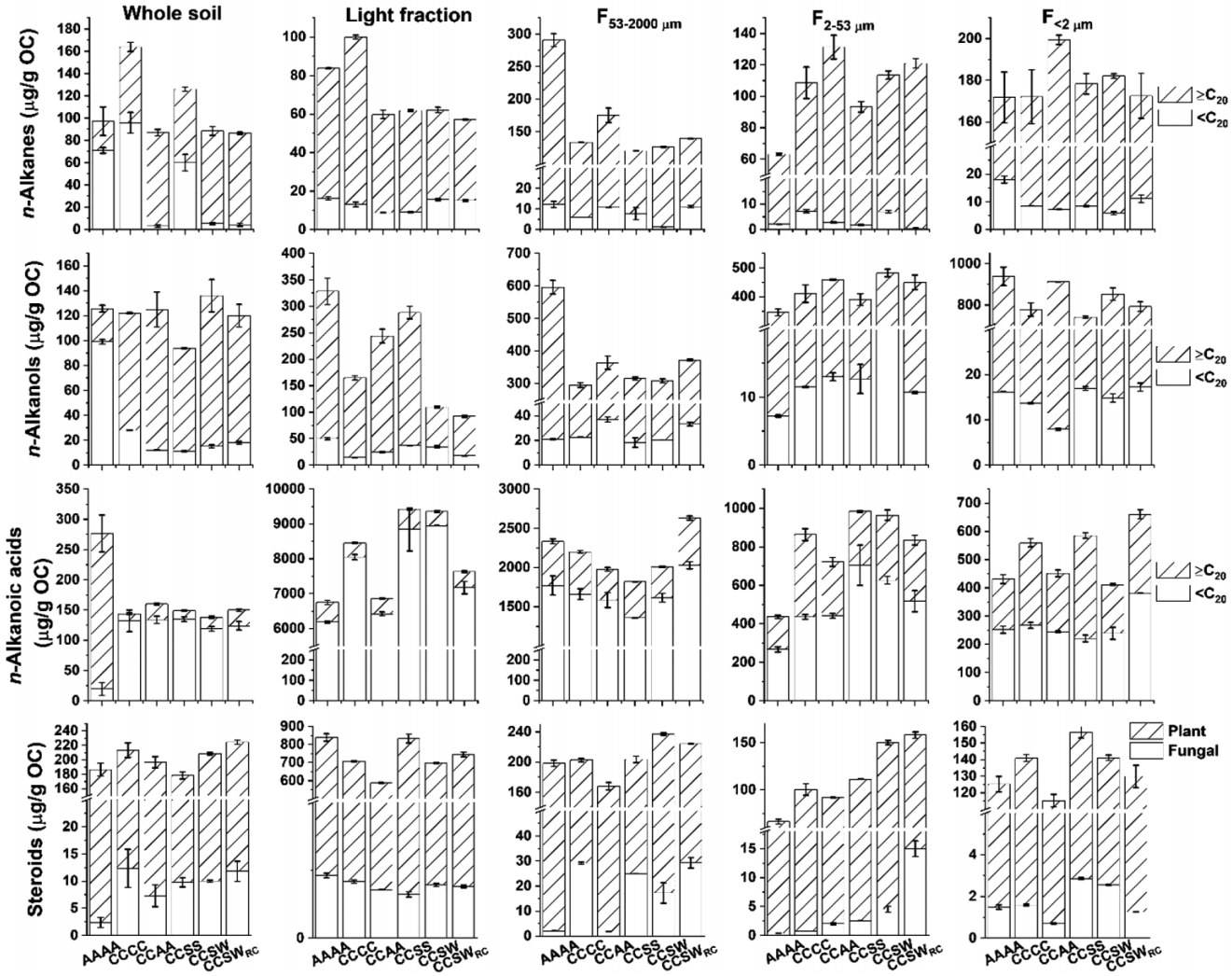

Otto and Simpson 2006b). The total concentration of lignin-derived phenols (sum of vanillyl, syringyl and cinnamyl compounds) decreased from light fraction, $F_{2–53\ \mu m}$, $F_{53–2000\ \mu m}$, to $F_{<2\ \mu m}$ (Fig. 3*d*). The total concentrations of lignin-derived phenols in the light fraction were similar to that of the whole soil (Fig. 3*d*). Positive correlations were observed between the total concentration of lignin-derived phenols in the unfractionated soil and light fraction, as well as in the soil and $F_{2–53\ \mu m}$ (Fig. A2). The distribution of phenols in different fractions across crop rotations was further examined using plots of syringyl/vanillyl versus cinnamyl/vanillyl phenols (Fig. 4). The ratios of syringyl/vanillyl and cinnamyl/vanillyl phenols have been used to assess the origin of lignin (i.e., gymnosperm or angiosperm wood, non-woody vascular plant tissues) (Ertel and Hedges 1984; Goñi et al. 2000; Otto and Simpson 2006b) and exhibit a range of lignin-derived phenol ratios (Fig. 4) that are consistent with non-woody angiosperm sources. Compared to the unfractionated soil, there was a greater separation of lignin-derived phenol distributions in fractions across crop rotations, especially in $F_{2–53\ \mu m}$ and $F_{<2\ \mu m}$ (Fig. 4). Relatively higher cinnamyl/vanillyl phenols ratios of samples from light fraction and $F_{53–2000\ \mu m}$ than the other two fractions were observed, but the syringyl/vanillyl phenols ratios were similar among fractions and with the whole soil (Fig. 4). Both oxidation state proxies ($(Ad/Al)_v$ and $(Ad/Al)_s$) decreased from $F_{<2\ \mu m}$, $F_{2–53\ \mu m}$, $F_{53–2000\ \mu m}$ to light fraction (Figs. 3*e* and 3*f*), except for the $F_{2–53\ \mu m}$ sample of CCSS. The degradation state of lignin-derived phenols of the unfractionated soil was at a similar level with $F_{2–53\ \mu m}$ for the majority of crop rotations (Figs. 3*e* and 3*f*). Within the

Fig. 2. The distribution of (*a*) cutin-derived compounds and (*b*) suberin-derived compounds concentrations (which were normalized to soil organic carbon content of whole soil or fraction), (*c*) cutin degradation state and (*d*) suberin/cutin ratio among varied crop rotational diversities in the whole soil (Man et al. 2021), light fraction, $F_{53–2000\ \mu m}$, $F_{2–53\ \mu m}$, and $F_{<2\ \mu m}$ (error bars indicate standard error, $n = 3$ for whole soil (Man et al. 2021) and $n = 2$ for fraction samples). AAAA, CCCC, CCAA, CCSS, CCSW, and $CCSW_{RC}$ represent continuous alfalfa, continuous corn, corn–corn–alfalfa–alfalfa, corn–corn–soybean–soybean, corn–corn–soybean–winter wheat, and corn–corn–soybean–winter wheat with red clover, respectively.

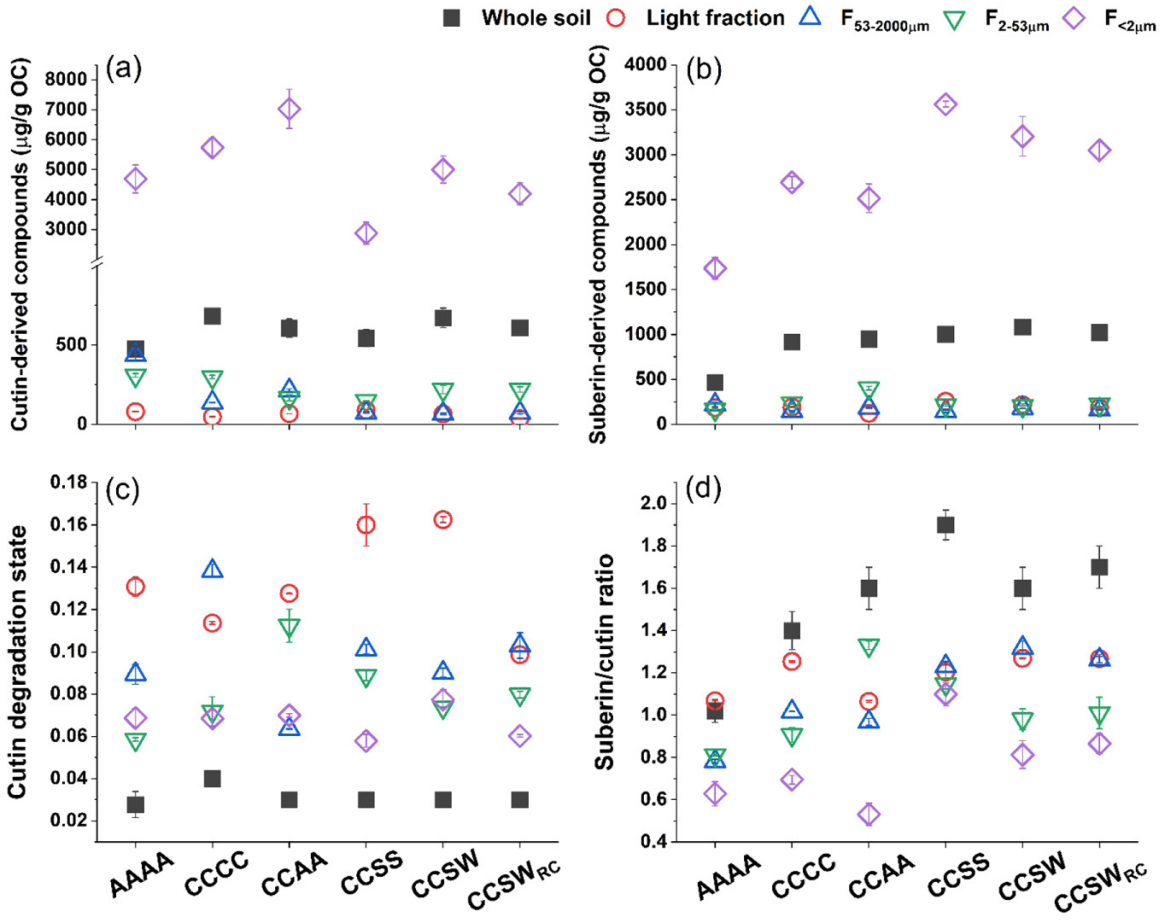

same soil fraction, lignin phenol distributions varied across crop rotations, especially between monoculture and diversified crop rotations (Fig. 4). Compared to monoculture treatments (AAAA and CCCC), the distributions of phenols (syringyl/vanillyl versus cinnamyl/vanillyl phenol ratios) from diversified crop rotations were less distinct from each other (Fig. 4). The total lignin-derived phenol concentrations were higher in relatively high diversified crop rotations (CCSW and $CCSW_{RC}$) than in low diversified crop rotations (AAAA, CCCC, CCAA, and CCSS) in light fraction, $F_{53–2000\ \mu m}$ and $F_{2–53\ \mu m}$ (Table 2). Both oxidation state proxies ($(Ad/Al)_v$ and $(Ad/Al)_s$) in $F_{2–53\ \mu m}$ were higher in low diversified crop rotations (Table 2).

Discussion

In this study, higher SOC concentrations were observed in light fractions and $F_{<2\ \mu m}$ compared to the whole soil (Table 1). The light fraction represents the biogeochemically active carbon pool where the SOM components are less protected and more readily available for decomposition (Six et al. 2002; Tonon et al. 2010; Poeplau et al. 2018; Haddix et al. 2020). In contrast, the mineral-associated fine fractions ($F_{2–53\ \mu m}$ and $F_{<2\ \mu m}$) contain carbon that is mainly stabilized via organo-mineral association (Jastrow et al. 2007; Sollins et al. 2009; Angst et al. 2017, 2018). In the light fractions and $F_{<2\ \mu m}$, higher SOC concentrations were observed in relatively high (more than two crop species) diversified crop rotations than in low diversified crop rotations (monoculture or two crop species, Table 2). These results suggest that the SOC concentration is enhanced with diversified crop rotations not just in the biogeochemically active carbon pool but also in the mineral-stabilized pool, which is consistent with the first hypothesis. The SOC concentrations in light fractions were significantly higher in relatively high crop rotational diversity than low diversity (Table 2). The SOC concentrations in light fractions also exhibited more variance across crop rotations (which were significantly different amongst crop rotations) than in other fractions (Table 1). These results indicate that the SOC concentrations in light fractions might be more sensitive to different crop rotations than in other fractions. This may be due to the enrichment of organic

Fig. 3. The concentrations (which were normalized to soil organic carbon content of whole soil or fraction) of (*a*) total cinnamyls, (*b*) total syringyls, (*c*) total vanillyls and (*d*) sum of three groups of lignin-derived phenols, and lignin-derived phenols degradation state of (*e*) vanillyl phenols and (*f*) syringyl phenols among varied crop rotational diversities in the whole soil (Man et al. 2021), light fractions, $F_{53–2000\ \mu m}$, $F_{2–53\ \mu m}$ and $F_{<2\ \mu m}$ (error bars indicate standard error, $n = 3$ for whole soil (Man et al. 2021) and $n = 2$ for fraction samples). AAAA, CCCC, CCAA, CCSS, CCSW, and $CCSW_{RC}$ represent continuous alfalfa, continuous corn, corn–corn–alfalfa–alfalfa, corn–corn–soybean–soybean, corn–corn–soybean–winter wheat, and corn–corn–soybean–winter wheat with red clover, respectively.

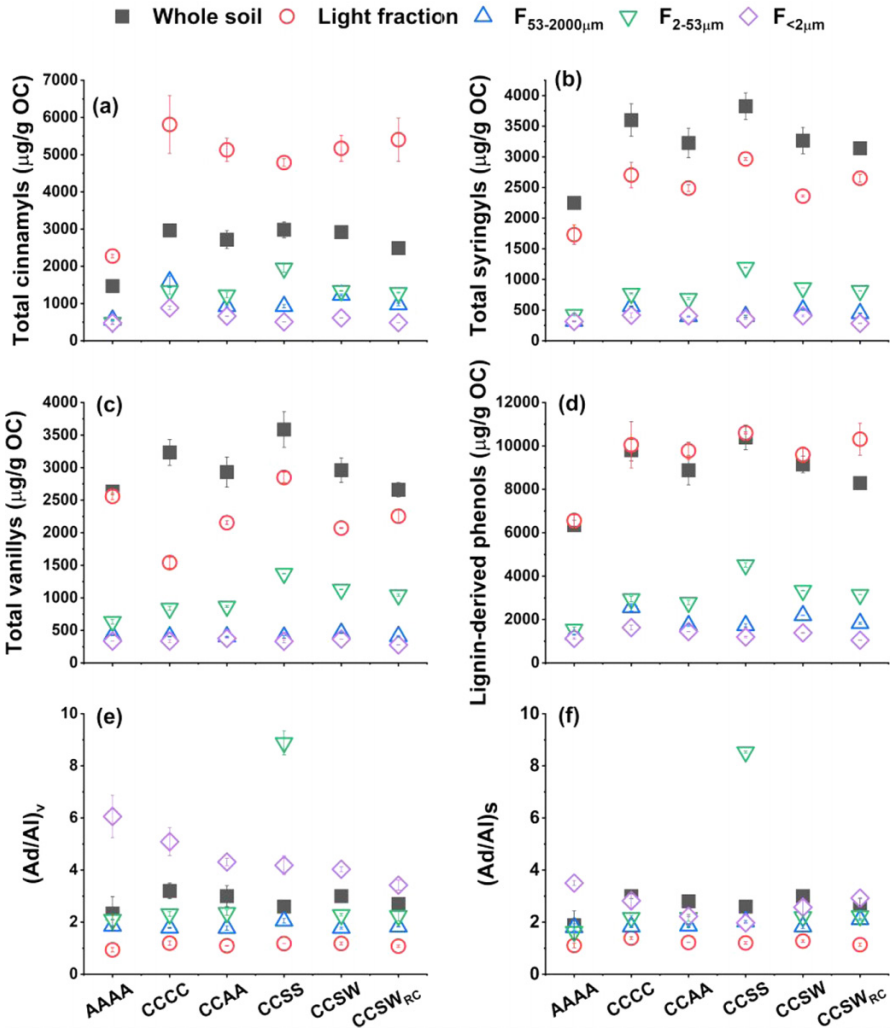

residues in light fractions which are in the early stages of decomposition and are not bound to minerals (Gregorich et al. 2006) and thus are more sensitive to crop input changes (Yang et al. 2012; Angst et al. 2018; Maiga et al. 2019; Zhang et al. 2020). Within stabilized carbon pools (mineral-associated fractions), targeted compound analyses showed increased concentrations of long-chain aliphatic compounds in fine fractions with relatively high crop rotational diversity. Positive linear correlations were observed between the concentrations of long-chain *n*-alkanols and *n*-alkanes ($\geq C_{20}$) in $F_{2–53\ \mu m}$ and soil, as well as between the concentration of suberin-derived and suberin- and cutin-derived compounds in $F_{<2\ \mu m}$ and soil (Fig. A2), suggesting that these components accumulate in fine aggregate sizes ($F_{2–53\ \mu m}$ and $F_{<2\ \mu m}$). These results are consistent with other studies that reported long-chain aliphatic compounds were preferentially stabilized in fine fractions (<53 μm) due to the strong association with soil minerals (Baldock et al. 1992; Guggenberger et al. 1995; Clemente et al. 2011). The study found higher concentrations of these specific groups of compounds with relatively highly diversified crop rotations in comparison to low diversification (Table 2), suggesting that crop rotational diversity likely enhanced the accumulation of long-chain aliphatic compounds in fine fractions. These groups of compounds persist longer in soil (Schmidt et al. 2011), which suggests that high crop rotational diversity may enhance SOC stability in the long-term.

When comparing the relatively high and low diversified crop rotations, greater contributions of aromatic and phenolic carbon were observed in relatively high (more than two crop species) diversified crop rotations across fractions with overall SOM composition analysis (Table 2); however,

Fig. 4. Plots of lignin distribution changed with varied crop rotations in different fractions (hallow symbols) compared with whole soil (Man et al. 2021) (solid symbols), where the error bars indicate standard error ($n = 3$ for whole soil (Man et al. 2021) and $n = 2$ for fraction samples); AAAA, CCCC, CCAA, CCSS, CCSW, and $CCSW_{RC}$ represent continuous alfalfa, continuous corn, corn–corn–alfalfa–alfalfa, corn–corn–soybean–soybean, corn–corn–soybean–winter wheat, and corn–corn–soybean–winter wheat with red clover, respectively.

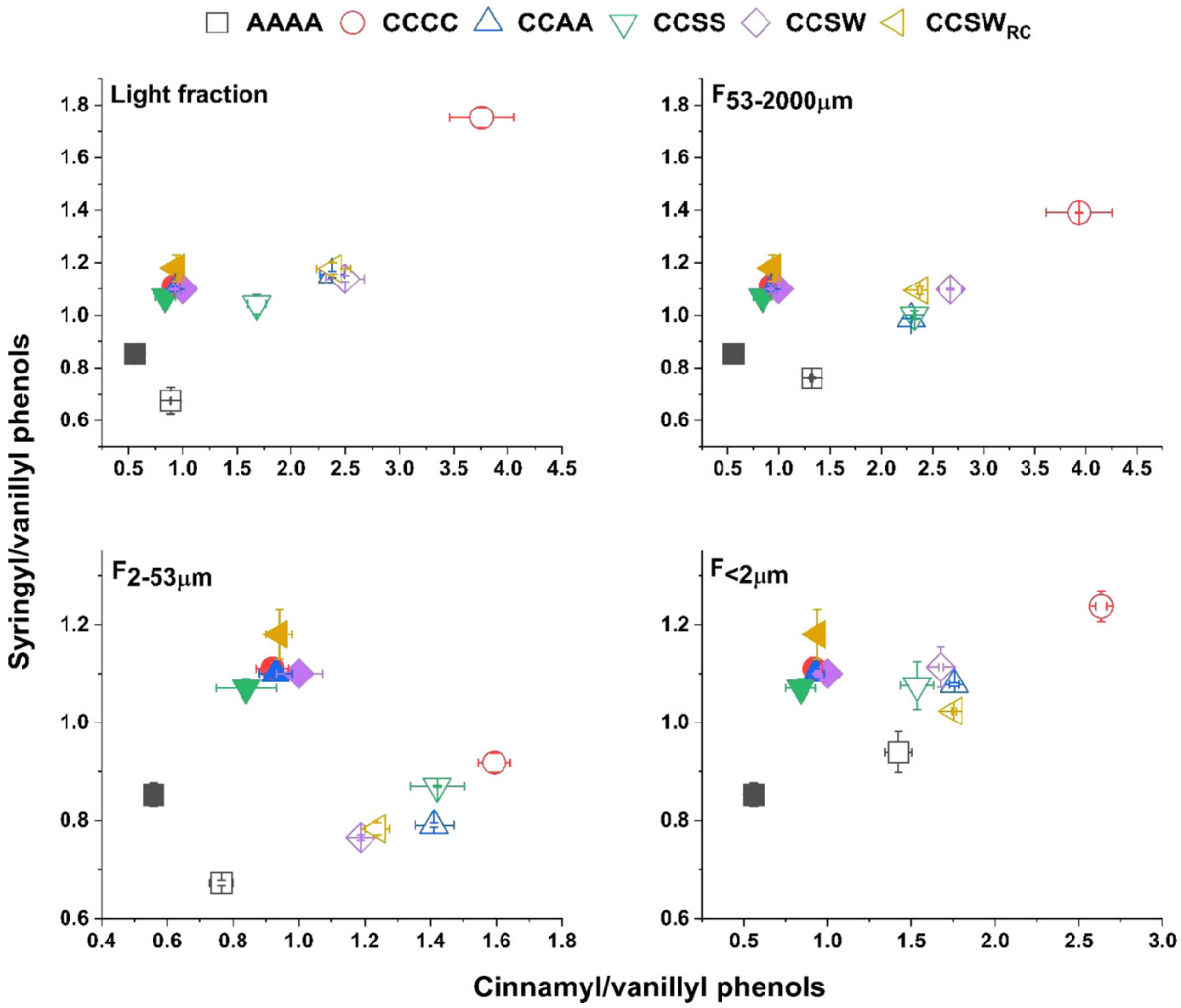

the difference was not significant ($P < 0.05$). This result partially supports the second hypothesis that higher crop rotational diversity is likely shifting SOM composition towards more aromatic groups (Audette et al. 2021), but larger sample sizes and further studies are needed to ascertain this change. Enhanced aromatic and phenolic carbon accumulation and preservation with relatively high crop rotational diversity were also observed with the targeted compound analysis of extractable phenols derived from lignin (Fig. 3). These lignin-derived phenols were mainly distributed in $F_{2–53\ \mu m}$ compared to other mineral-associated fractions (Fig. 3*d*) and the total concentrations of lignin-derived phenols in $F_{2–53\ \mu m}$ and in the unfractionated soil had a positive correlation (Fig. A2). In $F_{2–53\ \mu m}$, the higher concentrations of total lignin-derived phenols with lower oxidation states in relatively high diversified crop rotations (Table 2) indicate that higher crop rotational diversity may facilitate the accumulation of this group of compounds in soil (Audette et al. 2021). Some studies found that constantly adding plant inputs with different molecular compositions (i.e., relatively high crop rotational diversity (King et al. 2020)) enhanced soil microbial dynamics and substrate acquisition, which may help promote SOM functional complexity and preservation (McDaniel et al. 2014; Lehmann et al. 2020). Although the overall SOM degradation state (from ^{13}C NMR analysis) did not reveal differences between relatively high and low diversified crop rotations in this study, the distribution and degradation differences of specific SOM compounds were observed in fine fractions ($F_{2–53\ \mu m}$ and $F_{<2\ \mu m}$). These results suggest that the crop rotational diversity is likely to foster the specific accumulation of SOM components in fine mineral-associated fractions.

This study found that higher crop rotational diversity may increase soil carbon concentration and the accumulation of specific SOM components in soil fractions; meanwhile, the specific crop species (i.e., alfalfa and winter wheat) in the

rotation may also alter soil carbon stabilization (King and Blesh 2018; King et al. 2020; Man et al. 2021). For example, alfalfa may help enhance soil carbon storage in agroecosystems, which is likely due to the high ability of photosynthetically fixed carbon (King et al. 2020) and high root biomass inputs (Li et al. 2019; Song et al. 2021). In this study, higher SOC concentration was observed in AAAA in both unfractionated soil and mineral-associated fractions than in other crop rotations (Table 1). This suggests that alfalfa is likely to increase carbon sequestration in soil (Gregorich et al. 2001; Sanford et al. 2012; Jarecki et al. 2018; Poffenbarger et al. 2020). When comparing CCAA and CCSS (both contained two types of crops), CCAA had higher long-chain aliphatic lipids and suberin- and cutin-derived compounds concentrations in mineral-associated fractions ($F_{53–2000\ \mu m}$, $F_{2–53\ \mu m}$ and $F_{<2\ \mu m}$; Tables A2 and A3). This further suggests that alfalfa is likely to enhance the accumulation of specific SOM compounds in the mineral-stabilized carbon pools. Winter wheat, on the other hand, was also found to increase crop yield (Franzluebbers et al. 1994; Gagnon et al. 2019) and enhance SOC concentration due to deep root systems (Franzluebbers et al. 1994). However, increased mineral-associated SOC concentration in relatively high crop rotational diversity treatment in comparison to low diversification with and without winter wheat suggested that diversified crop rotation could be the main driver (Agomoh et al. 2021). In this study, the results indicated that the more diversified crop rotations (CCSW and $CCSW_{RC}$) may enhance the accumulation of stabilized SOM components. However, these crop rotations contained winter wheat, which may also contribute to the enhancement of root-derived SOM (suberin-derived aliphatic lipids) concentrations. Therefore, further studies are needed to assess whether the crop rotational diversity or including winter wheat in the crop rotation controls the accumulation of stabilized SOM.

Conclusions

This study used molecular-level analyses to assess the biogeochemistry differences of carbon (including SOC and specific SOM component concentrations, as well as SOM degradation states) in soil fractions with diversified crop rotations. The results suggested that diversified crop rotations may help enhance SOC concentration in the long-term, especially for relatively high crop rotational diversity (CCSW and $CCSW_{RC}$), where increased SOC concentrations in both light and mineral-associated fractions were observed. Accumulation of long-lived components (i.e., long-chain aliphatic lipids) in stabilized carbon pools (mineral-associated fractions) suggests that this practice may increase long-term SOC stability. These findings support our hypotheses that crop rotational diversity help to promote SOM stabilization in both active and stabilized carbon pools, thus may subsequently enhance soil stability and improve soil health and crop yields. The benefit of including alfalfa to build SOC was also confirmed from our results in which higher SOC concentrations and accumulation of long-chain aliphatic lipids in soil physical fractions were observed in crop rotations containing alfalfa. Overall, this study indicates that long-term diversified crop rotations may enhance SOM stability via the accumulation of longer-lived SOM components. Furthermore, our results demonstrate that soil carbon biogeochemical cycling in agroecosystems is altered uniquely by different crop rotation practices.

Acknowledgements

This research was supported by the Natural Sciences and Engineering Research Council (NSERC) of Canada Strategic Projects Grant. MJS is supported by NSERC via a Tier 1 Canada Research Chair in Integrative Molecular Biogeochemistry. We sincerely thank Dr. Ronald Soong for assistance with NMR acquisition.

Article information

History dates

Received: 12 April 2022
Accepted: 26 July 2022
Accepted manuscript online: 23 November 2022
Version of record online: 23 November 2022

Copyright

Data availability

Available upon request to corresponding author. An Appendix A with additional data are included with this submission.

Author information

Author ORCIDs

Meiling Man https://orcid.org/0000-0002-8982-5222
Myrna J. Simpson https://orcid.org/0000-0002-8084-411X

Author contributions

Huan Tong: conceptualization, data curation, formal analysis, investigation, methodology, validation, writing – original draft, writing – review & editing; Meiling Man: conceptualization, data curation, formal analysis, methodology, validation, writing – review & editing; Claudia Wagner-Riddle: conceptualization, funding acquisition, investigation, methodology, project administration, resources, writing – review & editing; Kari E. Dunfield: conceptualization, funding acquisition, project administration, resources, writing – review & editing; Bill Deen: conceptualization, methodology, resources, writing – review & editing; Myrna J. Simpson: conceptualization, funding acquisition, project administration, resources, supervision, writing – review & editing.

Conflict of interest

The authors have no conflicts of interest to declare that are relevant to the content of this article.

References

Agomoh, I.V., Drury, C.F., Yang, X., Phillips, L.A., and Reynolds, W.D. 2021. Crop rotation enhances soybean yields and soil health indicators. Soil Sci. Soc. Am. J. **85**: 1185–1195. doi:10.1002/saj2.20241.

Angeletti, C., Monaci, E., Giannetta, B., Polverigiani, S., and Vischetti, C. 2021. Soil organic matter content and chemical composition under two rotation management systems in a mediterranean climate. Pedosphere **31**: 903–911. doi:10.1016/S1002-0160(21)60032-2.

Angst, G., Mueller, K.E., Kögel-Knabner, I., Freeman, K.H., and Mueller, C.W., 2017. Aggregation controls the stability of lignin and lipids in clay-sized particulate and mineral associated organic matter. Biogeochemistry **132**: 307–324. doi:10.1007/s10533-017-0304-2.

Angst, G., Nierop, K.G.J., Angst, Š., and Frouz, J. 2018. Abundance of lipids in differently sized aggregates depends on their chemical composition. Biogeochemistry **140**: 111–125. doi:10.1007/s10533-018-0481-7.

Arshad, M.A., Soon, Y.K., and Ripmeester, J.A. 2011. Quality of soil organic matter and c storage as influenced by cropping systems in northwestern alberta, canada. Nutr. Cycl. Agroecosystems **89**: 71–79. doi:10.1007/s10705-010-9377-1.

Audette, Y., Congreves, K.A., Schneider, K., Zaro, G.C., Nunes, A.L.P., Zhang, H., and Voroney, R.P. 2021. The effect of agroecosystem management on the distribution of c functional groups in soil organic matter: a review. Biol. Fertil. Soils **57**: 881–894. doi:10.1007/s00374-021-01580-2. PMID: 34759437.

Bai, Z., Caspari, T., Gonzalez, M.R., Batjes, N.H., Mäder, P. Bünemann, E.K., et al. 2018. Effects of agricultural management practices on soil quality: a review of long-term experiments for europe and china. Agric. Ecosyst. Environ. **265**: 1–7. doi:10.1016/j.agee.2018.05.028.

Baldock, J.A., Oades, J.M., Waters, A.G., Peng, X., Vassallo, A.M., and Wilson, M.A. 1992. Aspects of the chemical structure of soil organic materials as revealed by solid-state13C NMR spectroscopy. Biogeochemistry **16**: 1–42. doi:10.1007/BF02402261.

Baldock, J.A., and Preston, C.M. 1995. Chemistry of carbon decomposition processes in forests as revealed by solid-state carbon-13 nuclear magnetic resonance. In Carbon Forms and Functions in Forest Soils. *Edited by* W.W. McFee, J.M. and Kelly. SSSA, Madison, WI, Pages 89–117.

Clemente, J.S., Simpson, A.J., and Simpson, M.J. 2011. Association of specific organic matter compounds in size fractions of soils under different environmental controls. Org. Geochem. **42**: 1169–1180. doi:10.1016/j.orggeochem.2011.08.010.

Congreves, K.A., Hayes, A., Verhallen, E.A., and Van Eerd, L.L. 2015. Long-term impact of tillage and crop rotation on soil health at four temperate agroecosystems. Soil Tillage Res. **152**: 17–28. doi:10.1016/j.still.2015.03.012.

Ertel, J.R., and Hedges, J.I. 1984. The lignin component of humic substances: distribution among soil and sedimentary humic, fulvic, and base-insoluble fractions. Geochim. Cosmochim. Acta **48**: 2065–2074. doi:10.1016/0016-7037(84)90387-9.

Franzluebbers, A.J., Hons, F.M., and Zuberer, D.A. 1994. Long-Term changes in soil carbon and nitrogen pools in wheat management systems. Soil Sci. Soc. Am. J. **58**: 1639–1645. doi:10.2136/sssaj1994.03615995005800060009x.

Freixo, A.A., Machado, P.L.O.D.A., Dos Santos, H.P., Silva, C.A., and Fadigas, F.D.S. 2002. Soil organic carbon and fractions of a rhodic ferralsol under the influence of tillage and crop rotation systems in southern brazil. Soil Tillage Res. **64**: 221–230. doi:10.1016/S0167-1987(01)00262-8.

Gagnon, B., Pouleur, S., Lafond, J., Parent, G., and Pageau, D. 2019. Agronomic and economic benefits of rotating corn with soybean and spring wheat under different tillage in eastern canada. Agron. J. **111**: 3109–3118. doi:10.2134/agronj2018.10.0653.

Garcia, R.A., Li, Y., and Rosolem, C.A. 2013. Soil organic matter and physical attributes affected by crop rotation under No-till. Soil Sci. Soc. Am. J. **77**: 1724–1731. doi:10.2136/sssaj2012.0310.

Goñi, M.A., and Hedges, J.I. 1990a. Potential applications of cutin-derived CuO reaction products for discriminating vascular plant sources in natural environments. Geochim. Cosmochim. Acta **54**: 3073–3081. doi:10.1016/0016-7037(90)90123-3.

Goñi, M.A., and Hedges, J.I. 1990b. The diagenetic behavior of cutin acids in buried conifer needles and sediments from a coastal marine environment. Geochim. Cosmochim. Acta **54**: 3083–3093. doi:10.1016/0016-7037(90)90124-4.

Goñi, M.A., Yunker, M.B., MacDonald, R.W., and Eglinton, T.I. 2000. Distribution and sources of organic biomarkers in arctic sediments from the mackenzie river and beaufort shelf. Mar. Chem. **71**: 23–51. doi:10.1016/S0304-4203(00)00037-2.

Gregorich, E.G., Beare, M.H., McKim, U.F., and Skjemstad, J.O. 2006. Chemical and biological characteristics of physically uncomplexed organic matter. Soil Sci. Soc. Am. J. **70**: 975–985. doi:10.2136/sssaj2005.0116.

Gregorich, E.G., Drury, C.F., and Baldock, J.A. 2001. Changes in soil carbon under long-term maize in monoculture and legume-based rotation. Can. J. Soil Sci. **81**: 21–31. doi:10.4141/S00-041.

Guggenberger, G., Zech, W., Haumaier, L., and Christensen, B.T. 1995. Land-use effects on the composition of organic matter in particle-size separates of soils: II. CPMAS and solution 13C NMR analysis. Eur. J. Soil Sci. **46**: 147–158. doi:10.1111/j.1365-2389.1995.tb01821.x.

Haddix, M.L., Gregorich, E.G., Helgason, B.L., Janzen, H., Ellert, B.H., and Francesca Cotrufo, M. 2020. Climate, carbon content, and soil texture control the independent formation and persistence of particulate and mineral-associated organic matter in soil. Geoderma **363**: 114160. doi:10.1016/j.geoderma.2019.114160.

Hedges, J.I., Blanchette, R.A., Weliky, K., and Devol, A.H. 1988. Effects of fungal degradation on the CuO oxidation products of lignin: a controlled laboratory study. Geochim. Cosmochim. Acta **52**: 2717–2726. doi:10.1016/0016-7037(88)90040-3.

Hedges, J.I., and Ertel, J.R. 1982. Characterization of lignin by gas capillary chromatography of cupric oxide oxidation products. Anal. Chem. **54**: 174–178. doi:10.1021/ac00239a007.

Helfrich, M., Ludwig, B., Buurman, P., and Flessa, H. 2006. Effect of land use on the composition of soil organic matter in density and aggregate fractions as revealed by solid-state 13C NMR spectroscopy. Geoderma **136**: 331–341. doi:10.1016/j.geoderma.2006.03.048.

Hermle, S., Anken, T., Leifeld, J., and Weisskopf, P. 2008. The effect of the tillage system on soil organic carbon content under moist, cold-temperate conditions. Soil Tillage Res. **98**: 94–105. doi:10.1016/j.still.2007.10.010.

Janovicek, K., Hooker, D., Weersink, A., Vyn, R., and Deen, B. 2021. Corn and soybean yields and returns are greater in rotations with wheat. Agron. J. **113**: 1691–1711. doi:10.1002/agj2.20605.

Jarecki, M., Grant, B., Smith, W., Deen, B., Drury, C. VanderZaag, A., et al. 2018. Long-term trends in corn yields and soil carbon under diversified crop rotations. J. Environ. Qual. **47**: 635–643. doi:10.2134/jeq2017.08.0317. PMID: 30025058.

Jastrow, J.D., Amonette, J.E., and Bailey, V.L. 2007. Mechanisms controlling soil carbon turnover and their potential application for enhancing carbon sequestration. Clim. Change **80**: 5–23. doi:10.1007/s10584-006-9178-3.

King, A.E., and Blesh, J. 2018. Crop rotations for increased soil carbon: perenniality as a guiding principle: perenniality. Ecol. Appl. **28**: 249–261. doi:10.1002/eap.1648. PMID: 29112790.

King, A.E., Congreves, K.A., Deen, B., Dunfield, K.E., Simpson, M.J., Voroney, R.P., and Wagner-Riddle, C. 2020. Crop rotations differ in soil carbon stabilization efficiency, but the response to quality of structural plant inputs is ambiguous. Plant Soil **457**: 207–224. doi:10.1007/s11104-020-04728-5.

Kögel-Knabner, I. 1997. 13C and 15 N NMR spectroscopy as a tool in soil organic matter studies. Geoderma **80**: 243–270. doi:10.1016/S0016-7061(97)00055-4.

Lajtha, K., Bowden, R.D., and Nadelhoffer, K. 2014. Litter and root manipulations provide insights into soil organic matter dynamics and stability. Soil Sci. Soc. Am. J. **78**: S261. doi:10.2136/sssaj2013.08.0370nafsc.

Lal, R. 2004. Soil carbon sequestration impacts on global climate change and food security. Science (80-.), **304**: 1623–1627. doi:10.1126/science.1097396.

Lange, M., Eisenhauer, N., Sierra, C.A., Bessler, H., Engels, C. Griffiths, R.I., et al. 2015. Plant diversity increases soil microbial activity and soil carbon storage. Nat. Commun. 2015 61 **6**: 1–8. doi:10.1038/ncomms7707.

Lehmann, J., Hansel, C.M., Kaiser, C., Kleber, M., Maher, K. Manzoni, S., et al. 2020. Persistence of soil organic carbon caused by functional complexity. Nat. Geosci. **13**: 529–534. doi:10.1038/s41561-020-0612-3.

Li, J., Ramirez, G.H., Kiani, M., Quideau, S., Smith, E. Janzen, H., et al. 2018. Soil organic matter dynamics in long-term temperate agroecosystems: rotation and nutrient addition effects. Can. J. Soil Sci. **98**: 232–245. doi:10.1139/cjss-2017-0127.

Li, Q., Zhou, D., Denton, M.D., and Cong, S. 2019. Alfalfa monocultures promote soil organic carbon accumulation to a greater extent than perennial grass monocultures or grass-alfalfa mixtures. Ecol. Eng. **131**: 53–62. doi:10.1016/j.ecoleng.2019.03.002.

Maiga, A., Alhameid, A., Singh, S., Polat, A., Singh, J., Kumar, S., and Osborne, S. 2019. Responses of soil organic carbon, aggregate stability, carbon and nitrogen fractions to 15 and 24 years of no-till diversified crop rotations. Soil Res. **57**: 149–157. CSIRO. doi:10.1071/SR18068.

Man, M., Wagner-Riddle, C., Dunfield, K.E., Deen, B., and Simpson, M.J. 2021. Long-term crop rotation and different tillage practices alter soil organic matter composition and degradation. Soil Tillage Res. **209**: 104960. doi:10.1016/j.still.2021.104960.

McDaniel, M.D., Grandy, A.S., Tiemann, L.K., and Weintraub, M.N. 2014. Crop rotation complexity regulates the decomposition of high and low quality residues. Soil Biol. Biochem. **78**: 243–254. doi:10.1016/j.soilbio.2014.07.027.

Mitchell, P., Simpson, A., Soong, R., and Simpson, M. 2018. Nuclear magnetic resonance analysis of changes in dissolved organic matter composition with successive layering on clay mineral surfaces. Soil Syst. **2**: 8. doi:10.3390/soils2010008.

Moreira, R.S., Chiba, M.K., De Maria, I.C., Siqueira, C.C.Z., Duarte, A.P., and Milori, D.M.B.P. 2018. Role of crop rotations in the dynamic of soil organic matter pools. J. Agric. Sci. **10**: 341.

Ogle, S.M., Jay Breidt, F., Eve, M.D., and Paustian, K. 2003. Uncertainty in estimating land use and management impacts on soil organic carbon storage for US agricultural lands between 1982 and 1997. Glob. Chang. Biol. **9**: 1521–1542. doi:10.1046/j.1365-2486.2003.00683.x.

Otto, A., and Simpson, M.J. 2005. Degradation and preservation of vascular plant-derived biomarkers in grassland and forest soils from western canada. Biogeochemistry **74**: 377–409. doi:10.1007/s10533-004-5834-8.

Otto, A., and Simpson, M.J. 2006a. Sources and composition of hydrolysable aliphatic lipids and phenols in soils from western canada. Org. Geochem. **37**: 385–407. doi:10.1016/j.orggeochem.2005.12.011.

Otto, A., and Simpson, M.J. 2006b. Evaluation of CuO oxidation parameters for determining the source and stage of lignin degradation in soil. Biogeochemistry **80**: 121–142. doi:10.1007/s10533-006-9014-x.

Paustian, K., Six, J., Elliott, E.T., and Hunt, H.W. 2000. Management options for reducing CO2 emissions from agricultural soils. Biogeochemistry **48**: 147–163. doi:10.1023/A:1006271331703.

Pinto, P.C.R., Da Silva, E.A.B., and Rodrigues, A.E. 2010. Comparative study of solid-phase extraction and liquid-liquid extraction for the reliable quantification of high value added compounds from oxidation processes of wood-derived lignin. Ind. Eng. Chem. Res. **49**: 12311–12318. American Chemical Society. doi:10.1021/ie101680s.

Poeplau, C., Don, A., Six, J., Kaiser, M., Benbi, D. Chenu, C., et al. 2018. Isolating organic carbon fractions with varying turnover rates in temperate agricultural soils – a comprehensive method comparison. Soil Biol. Biochem. **125**: 10–26. doi:10.1016/j.soilbio.2018.06.025.

Poffenbarger, H.J., Olk, D.C., Cambardella, C., Kersey, J., Liebman, M. Mallarino, A., et al. 2020. Whole-profile soil organic matter content, composition, and stability under cropping systems that differ in belowground inputs. Agric. Ecosyst. Environ. **291**: 106810. doi:10.1016/j.agee.2019.106810.

Preston, C.M., Trofymow, J.A., Sayer, B.G., and Niu, J. 1997. 13C nuclear magnetic resonance spectroscopy with cross-polarization and magic-angle spinning investigation of the proximate-analysis fractions used to assess litter quality in decomposition studies. Can. J. Bot. **75**: 1601–1613. doi:10.1139/b97-872.

Reeves, D.W. 1997. The role of soil organic matter in maintaining soil quality in continuous cropping systems. Soil Tillage Res., **43**: 131–167. doi:10.1016/S0167-1987(97)00038-X.

Ren, C., Wang, T., Xu, Y., Deng, J., Zhao, F. Yang, G., et al. 2018. Differential soil microbial community responses to the linkage of soil organic carbon fractions with respiration across land-use changes. For. Ecol. Manage. **409**: 170–178. doi:10.1016/j.foreco.2017.11.011.

Saidy, A.R., Smernik, R.J., Baldock, J.A., Kaiser, K., and Sanderman, J. 2013. The sorption of organic carbon onto differing clay minerals in the presence and absence of hydrous iron oxide. Geoderma **209–210**: 15–21. doi:10.1016/j.geoderma.2013.05.026.

Sanford, G.R., Posner, J.L., Jackson, R.D., Kucharik, C.J., Hedtcke, J.L., and Lin, T.L. 2012. Soil carbon lost from mollisols of the north central U.S.A. with 20 years of agricultural best management practices. Agric. Ecosyst. Environ. **162**: 68–76. doi:10.1016/j.agee.2012.08.011.

Savarese, C., Drosos, M., Spaccini, R., Cozzolino, V., and Piccolo, A. 2021. Molecular characterization of soil organic matter and its extractable humic fraction from long-term field experiments under different cropping systems. Geoderma **383**: 114700. doi:10.1016/j.geoderma.2020.114700.

Schmidt, M.W.I., Knicker, H., Hatcher, P.G., and Kögel-Knabner, I. 1997. Improvement of 13C and 15 N CPMAS NMR spectra of bulk soils, particle size fractions and organic material by treatment with 10% hydrofluoric acid. Eur. J. Soil Sci. **48**: 319–328. doi:10.1111/j.1365-2389.1997.tb00552.x.

Schmidt, M.W.I., Torn, M.S., Abiven, S., Dittmar, T., Guggenberger, G. Janssens, I.A., et al. 2011. Persistence of soil organic matter as an ecosystem property. Nature **478**: 49–56. doi:10.1038/nature10386. PMID: 21979045.

Simpson, M.J., Otto, A., and Feng, X. 2008. Comparison of solid-state carbon-13 nuclear magnetic resonance and organic matter biomarkers for assessing soil organic matter degradation. Soil Sci. Soc. Am. J. **72**: 268–276. doi:10.2136/sssaj2007.0045.

Simpson, M.J., and Simpson, A.J. 2012. The chemical ecology of soil organic matter molecular constituents. J. Chem. Ecol. **38**: 768–784. doi:10.1007/s10886-012-0122-x. PMID: 22549555.

Six, J., Conant, R.T., Paul, E.A., and Paustian, K. 2002. Stabilization mechanisms of SOM implications for c saturation of soils.pdf. Plant Soil **241**: 155–176. doi:10.1023/A:1016125726789.

Sollins, P., Kramer, M.G., Swanston, C., Lajtha, K., Filley, T. Aufdenkampe, A.K., et al. 2009. Sequential density fractionation across soils of contrasting mineralogy: evidence for both microbial- and mineral-controlled soil organic matter stabilization. Biogeochemistry **96**: 209–231. doi:10.1007/s10533-009-9359-z.

Soman, C., Li, D., Wander, M.M., and Kent, A.D. 2017. Long-term fertilizer and crop-rotation treatments differentially affect soil bacterial community structure. Plant Soil **413**: 145–159. doi:10.1007/s11104-016-3083-y.

Song, X., Fang, C., Yuan, Z.Q., and Li, F.M. 2021. Long-Term growth of alfalfa increased soil organic matter accumulation and nutrient mineralization in a semi-arid environment. Front. Environ. Sci. **9**: 91. doi:10.3389/fenvs.2021.649346.

Soon, Y.K., Arshad, M.A., Haq, A., and Lupwayi, N. 2007. The influence of 12 years of tillage and crop rotation on total and labile organic carbon in a sandy loam soil. Soil Tillage Res. **95**: 38–46. doi:10.1016/j.still.2006.10.009.

Srivastava, P., Singh, R., Bhadouria, R., Tripathi, S., Singh, H., and Raghubanshi, A.S. 2019. Understanding soil aggregate dynamics and its relation with land use and climate change. *In* Climate Change and Agricultural Ecosystems. Elsevier, Pages 331–354.

Tonon, G., Sohi, S., Francioso, O., Ferrari, E., Montecchio, D. Gioacchini, P., et al. 2010. Effect of soil pH on the chemical composition of organic matter in physically separated soil fractions in two broadleaf woodland sites at rothamsted, uK. Eur. J. Soil Sci. **61**: 970–979. doi:10.1111/j.1365-2389.2010.01310.x.

West, T.O., and Post, W.M. 2002. Soil organic carbon sequestration rates by tillage and crop rotation. Soil Sci. Soc. Am. J. **66**: 1930. doi:10.2136/sssaj2002.1930.

Yang, X., Ren, W., Sun, B., and Zhang, S. 2012. Effects of contrasting soil management regimes on total and labile soil organic carbon fractions in a loess soil in china. Geoderma **177–178**: 49–56. doi:10.1016/j.geoderma.2012.01.033.

Yang, Z., Liao, Y., Fu, X., Zaporski, J., Peters, S. Jamison, M., et al. 2019. Temperature sensitivity of mineral-enzyme interactions on the hydrolysis of cellobiose and indican by β-glucosidase. Sci. Total Environ. **686**: 1194–1201. doi:10.1016/j.scitotenv.2019.05.479. PMID: 31412515.

Zhang, Y., Li, X., Gregorich, E., McLaughlin, N., Zhang, X. Guo, Y., et al. 2020. Tillage and cropping effects on soil organic carbon: biodegradation and storage in density and size fractions. Eur. J. Soil Sci. **71**: 1188–1199.

Zhao, N., Yang, X., Huang, G., Lv, Y., Zhang, J. Fan, Y., et al. 2021. Chemical and spectroscopic characteristics of humic acid from a clay loam soil in ontario after 52 years of consistent fertilization and crop rotation. Pedosphere **31**: 204–213. doi:10.1016/S1002-0160(20)60019-4.

Zotarelli, L., Alves, B.J.R.J.R., Urquiaga, S., Boddey, R.M.M., and Six, J. 2007. Impact of tillage and crop rotation on light fraction and intra-aggregate soil organic matter in two oxisols. Soil Tillage Res. **95**: 196–206. doi:10.1016/j.still.2007.01.002.

Appendix A

Detailed sequential extraction procedure

Soil fractions (light fraction 0.2 g; $F_{53–2000\ \mu m}$ and $F_{2–53\ \mu m}$ 15 g and $F_{<2\ \mu m}$ 3 g) were weighed into 50 mL Teflon tubes and then sonicated with 30 mL of dichloromethane, dichloromethane and methanol mixture (1:1 by volume), and methanol (each for 15 min). Then the combined solvent extracts were filtered through GF/A and GF/F glass filters (Whatman, Kent, UK) and concentrated by rotary evaporation. The concentrated extracts were further dried with nitrogen (N_2) gas in 2 mL glass vials (Otto and Simpson 2005). Air-dried solvent extracted samples were then base hydrolyzed with 20 mL of methanolic potassium hydroxide (KOH, 1 M in methanol) solution in Teflon lined bombs at 100 °C for 3 h. The samples were sonicated twice with a mixture of 15 mL dichloromethane and methanol (1:1 by volume). The combined extracts were centrifuged, and the supernatants were acidified to pH 1 with hydrochloric acid (HCl, 6 M in deionized water) and rotary evaporated. The solution was then liquid-liquid extracted three times with 30 mL of diethyl ether. The combined extracts were dried with anhydrous sodium sulphate (Na_2SO_4), concentrated by rotary evaporation, and evaporated to dryness under N_2 gas in 2 mL glass vials (Goñi and Hedges 1990b; Otto and Simpson 2006a). The base hydrolyzed samples were then oxidized with 1 g CuO, 100 mg ammonium iron (II) sulphate hexahydrate [$Fe(NH_4)_2(SO_4)_2{\cdot}6H_2O$] and 15 mL of sodium hydroxide (NaOH, 2 M in deionized water) in Teflon lined bombs at 170 °C for 2.5 h. The extracts were acidified to the pH of 1 with 6 M HCl and kept at room temperature in the dark for 1 h to prevent the polymerization of cinnamic acids (Hedges and Ertel 1982; Hedges et al. 1988; Otto and Simpson 2006b). Then the supernatants were solid-phase extracted using HLB SPE cartridges (Waters Limited, Mississauga, ON, Canada) and eluted with 0.5 mL of dichloromethane, methyl acetate and pyridine mixture (70:25:5 by volume, three times) followed by two × 0.5 mL of methanol (Kaiser and Benner 2012). The extracts were dried with anhydrous Na_2SO_4, concentrated by rotary evaporation, and dried under N_2 gas in 2 mL glass vials.

Table A1. The soil fractionation yields and the soil organic carbon (SOC) concentration in fractions with the unit g OC/kg soil.

	Light fraction	$F_{53–2000\,\mu m}$	$F_{2–53\,\mu m}$	$F_{<2\,\mu m}$	Recovery (%)
Continuous alfalfa					
Fraction yield (%)	0.3	40.7	43.9	12.1	97.0
SOC concentration (g/kg)	1.0 ± 0.0a	8.4 ± 0.2a	7.1 ± 0.1a	7.9 ± 0.1c	93.7
Continuous corn					
Fraction yield (%)	0.3	33.1	50.1	13.8	97.3
SOC concentration (g/kg)	0.8 ± 0.0b	5.4 ± 0.2b	5.2 ± 0.1b	7.9 ± 0.2c	85.6
Corn–corn–alfalfa–alfalfa					
Fraction yield (%)	0.2	30.8	50.5	15.7	97.2
SOC concentration (g/kg)	0.6 ± 0.0e	5.9 ± 0.3b	5.5 ± 0.1b	8.8 ± 0.1b	87.4
Corn–corn–soybean–soybean					
Fraction yield (%)	0.3	29.6	52.7	15.2	97.8
SOC concentration (g/kg)	0.6 ± 0.0e	5.1 ± 0.2b	4.9 ± 0.5b,c	7.8 ± 0.3b,c	94.5
Corn–corn–soybean–winter wheat					
Fraction yield (%)	0.2	34.9	47.3	15.3	97.7
SOC concentration (g/kg)	0.7 ± 0.0c	5.1 ± 0.3b	4.2 ± 0.0c	8.6 ± 0.1b,c	88.1
Corn–corn–soybean–winter wheat with red clover					
Fraction yield (%)	0.2	28.2	53.2	15.8	97.4
SOC concentration (g/kg)	0.7 ± 0.0d	5.4 ± 0.1b	4.7 ± 0.2b,c	9.7 ± 0.1a	93.8

Note : SOC concentration of the sample is significantly different from other crop rotation treatments within same soil fraction at $P < 0.05$; significant differences between every two treatments are represented by different letters. SOC concentration was determined based on the SOC values measured in the fractions (Table 1) multiply the mass yield of each fraction.

Table A2. Solvent extractable compound concentrations (which were normalized to soil organic carbon (OC) concentration of fractions, μg/g OC) from four fractions within crop rotation treatments (continuous alfalfa (AAAA), continuous corn (CCCC), corn–corn–alfalfa–alfalfa (CCAA), corn–corn–soybean–soybean (CCSS), corn–corn–soybean–winter wheat (CCSW) and corn–corn–soybean–winter wheat with red clover ($CCSW_{RC}$)) (mean ± standard error; $n = 2$).

	AAAA	CCCC	CCAA	CCSS	CCSW	$CCSW_{RC}$
Light fraction						
Short-chain *n*-alkanes (<C_{20})	16.2 ± 0.9a,b	13.0 ± 1.2a,b,c	8.8 ± 0.0a,c	9.1 ± 0.4c	15.7 ± 0.6a,b	15.1 ± 0.4b
Long-chain *n*-alkanes (≥C_{20})	67.6 ± 0.3b	86.9 ± 1.0a	51.0 ± 2.2c,d	52.8 ± 0.4c	46.5 ± 1.4d	42.0 ± 0.2d
Total *n*-alkanes	83.7 ± 1.2b	100.0 ± 2.2a	59.8 ± 2.1c,d	61.8 ± 0.8c	62.2 ± 0.8c	57.1 ± 0.2d
Short-chain *n*-alkanols (<C_{20})	50.0 ± 2.2a	14.7 ± 0.4d	25.1 ± 1.0c	37.3 ± 0.3b	34.7 ± 2.1b,c	17.5 ± 0.3e
Long-chain *n*-alkanols (≥C_{20})	278.4 ± 25.1a,c	150.2 ± 3.8b	218.7 ± 13.0a	250.7 ± 11.8a	74.9 ± 1.8c	74.9 ± 2.0c
Total *n*-alkanols	328.4 ± 27.2a	164.9 ± 4.3b	243.8 ± 11.9a	288.0 ± 12.1a	109.6 ± 3.9c	92.4 ± 2.3c
Short-chain *n*-alkanoic acids (<C_{20})	6187.0 ± 29.8a,d	8048.6 ± 75.3a	6421.4 ± 55.4c,d	8844.2 ± 619.3a,b,d	8951.3 ± 5.4a,b	7173.3 ± 178.5b,c
Long-chain *n*-alkanoic acids (≥C_{20})	564.7 ± 61.2a,b	400.9 ± 20.2b	435.3 ± 23.2a,b	580.5 ± 28.3a	406.2 ± 32.5a,b	460.3 ± 22.1a,b
Total *n*-alkanoic acids	6751.7 ± 91.0c	8449.5 ± 95.4b	6856.8 ± 78.6c	9424.7 ± 591.0a,b	9357.5 ± 27.1a	7633.6 ± 200.6b,c
Short-chain aliphatic lipids[a]	6253.1 ± 32.8c	8076.3 ± 77.0a	6455.4 ± 56.4b,c	8890.5 ± 618.6a,b,c	9001.7 ± 3.9a,b	7205.9 ± 178.5b
Long-chain aliphatic lipids[b]	910.7 ± 86.6a,b,c	638.1 ± 25.0b,c	705.0 ± 12.4a,b	884.0 ± 40.5a	527.5 ± 35.6c	577.2 ± 24.3c
Fungal-derived steroids[c]	9.2 ± 0.3a,b	8.3 ± 0.3b	7.1 ± 0.0a	6.4 ± 0.4b	7.8 ± 0.2a,b	7.6 ± 0.2a,b
Plant-derived steroids[d]	830.2 ± 20.5a	700.0 ± 3.5b	579.1 ± 2.8c	827.0 ± 24.3a	691.2 ± 2.8b	737.5 ± 12.6a,b
Cyclic lipids[e]	936.0 ± 25.5a,c	737.3 ± 0.9c	689.4 ± 9.3d	853.5 ± 24.6a,b,c	769.6 ± 3.3a,b	809.8 ± 15.5a
$F_{53–2000\ \mu m}$ fraction						
Short-chain *n*-alkanes (<C_{20})	12.2 ± 1.6a,b,c	6.0 ± 0.0b	10.9 ± 0.1a	7.8 ± 2.9a,b,c	1.4 ± 0.1c	11.2 ± 0.6a,b
Long-chain *n*-alkanes (≥C_{20})	278.5 ± 9.9a	127.6 ± 0.0b,c	164.3 ± 11.0b,c,d	112.8 ± 0.3d	125.2 ± 0.5c	128.3 ± 0.5b
Total *n*-alkanes	290.7 ± 11.5a	133.6 ± 0.1b,d	175.2 ± 10.9b,c	120.6 ± 2.7c,d	126.5 ± 0.6c	139.5 ± 1.1b
Short-chain *n*-alkanols (<C_{20})	20.8 ± 0.5b	22.5 ± 0.2b,c	37.0 ± 2.0a	18.3 ± 3.9a,b,c	20.3 ± 0.0b,c	33.2 ± 1.5a
Long-chain *n*-alkanols (≥C_{20})	575.2 ± 20.8a	272.4 ± 7.1c	326.7 ± 20.5b,c	297.1 ± 4.4c	287.7 ± 6.1c	338.6 ± 3.6b
Total *n*-alkanols	595.9 ± 21.3a	294.9 ± 7.3c	363.7 ± 22.6b,c	315.4 ± 0.5c	308.1 ± 6.0c	371.8 ± 2.1b
Short-chain *n*-alkanoic acids (<C_{20})	1771.7 ± 121.0a,b	1661.3 ± 68.9b	1587.2 ± 95.0a,b	1358.5 ± 0.7b	1614.9 ± 53.7b	2027.8 ± 44.0a
Long-chain *n*-alkanoic acids (≥C_{20})	560.8 ± 31.2a	537.8 ± 16.2a,b	389.7 ± 23.8c	460.4 ± 0.6a,b,c	394.6 ± 8.1c	604.8 ± 26.0a,b
Total *n*-alkanoic acids	2332.5 ± 89.7a,b	2199.1 ± 85.1a,b	1976.9 ± 118.8b	1818.9 ± 0.1b	2009.4 ± 61.8b	2632.6 ± 70.0a
Short-chain aliphatic lipids[a]	1804.7 ± 123.1a,b,c	1689.7 ± 69.1b,c	1635.0 ± 96.9a,c	1384.6 ± 7.5b	1636.6 ± 53.8b,c	2072.1 ± 41.9a
Long-chain aliphatic lipids[b]	1414.4 ± 0.5a	937.8 ± 23.3b,c	880.8 ± 55.3a,b,c	870.4 ± 5.2b	807.5 ± 2.5c	1071.7 ± 29.1a,b
Fungal-derived steroid[c]	2.1 ± 0.0b,c	29.2 ± 0.5a	1.8 ± 0.1b	25.0 ± 0.0a	17.2 ± 4.1a,b,c	29.3 ± 2.1a
Plant-derived steroids[d]	196.4 ± 4.2b	173.5 ± 2.2c	166.2 ± 4.8c	178.6 ± 4.1b,c	220.2 ± 1.8a	194.9 ± 0.7b
Cyclic lipids[e]	234.5 ± 1.0b	221.4 ± 2.4c,e	189.8 ± 5.8d	227.4 ± 1.0c	290.2 ± 5.4a	248.7 ± 4.4b
$F_{2–53\ \mu m}$ fraction						
Short-chain *n*-alkanes (<C_{20})	2.1 ± 0.1a,c	7.2 ± 0.6a	2.7 ± 0.3c	1.8 ± 0.1a,b,c	7.0 ± 0.5b	0.6 ± 0.0a,c
Long-chain *n*-alkanes (≥C_{20})	61.0 ± 0.7d	101.5 ± 10.0b	128.6 ± 7.6a,b	91.4 ± 3.3c	106.6 ± 2.6a	120.4 ± 3.0b
Total *n*-alkanes	63.1 ± 0.7e	108.6 ± 10.6b	131.4 ± 7.9a,b	93.3 ± 3.2c	113.6 ± 3.2c,d	121.0 ± 3.0a
Short-chain *n*-alkanols (<C_{20})	7.2 ± 0.2c	11.5 ± 0.1b,c	13.0 ± 0.6a	12.7 ± 2.1a,b,c	20.0 ± 0.5c,d	10.7 ± 0.2a

Table A2. (*concluded*).

	AAAA	CCCC	CCAA	CCSS	CCSW	$CCSW_{RC}$
Long-chain *n*-alkanols ($\geq C_{20}$)	338.9 ± 12.2c	399.4 ± 30.3a	446.6 ± 2.4a,b	377.2 ± 20.6a	461.9 ± 13.3a	439.4 ± 25.1b
Total *n*-alkanols	346.1 ± 12.1c	411.0 ± 30.2a	459.6 ± 3.0a	389.9 ± 18.5a,b	481.9 ± 13.8a	450.1 ± 24.9b
Short-chain *n*-alkanoic acids ($<C_{20}$)	267.2 ± 13.2c	435.7 ± 12.7b	441.8 ± 12.2b	704.4 ± 104.1a,b,c	626.4 ± 19.9a	517.9 ± 54.9a,b
Long-chain *n*-alkanoic acids ($\geq C_{20}$)	169.0 ± 8.2a,d	427.5 ± 30.8a,c	280.1 ± 22.6b,d	279.8 ± 5.2d	337.8 ± 27.0b	317.1 ± 24.6a,c
Total *n*-alkanoic acids	436.2 ± 21.4b,c	863.2 ± 43.6b,c	721.9 ± 34.7a,b	984.1 ± 98.8a	964.3 ± 46.8a,b	834.9 ± 79.5c
Short-chain aliphatic lipids[a]	276.5 ± 13.1c	454.4 ± 13.2b	457.6 ± 12.5b	718.9 ± 106.3a,b,c	653.4 ± 20.9a	529.2 ± 54.8a,b
Long-chain aliphatic lipids[b]	568.9 ± 21.1b	928.4 ± 71.2a	855.3 ± 17.4a	748.4 ± 29.2a	906.3 ± 42.9a	876.8 ± 52.6a
Fungal-derived steroid[c]	0.4 ± 0.0b	0.8 ± 0.0c	2.0 ± 0.2b	2.6 ± 0.0a	4.5 ± 0.5a,b,c	15.0 ± 1.4a,c
Plant-derived steroids[d]	66.1 ± 2.4b	99.6 ± 6.1c	89.9 ± 0.3c	108.8 ± 0.3b,c	145.6 ± 2.4a	143.0 ± 3.4b
Cyclic lipids[e]	77.4 ± 2.0a	108.3 ± 5.9c,d	101.3 ± 0.3d	124.8 ± 1.4c	169.6 ± 3.3b	173.7 ± 3.7a
$F_{<2\ \mu m}$ fraction						
Short-chain *n*-alkanes ($<C_{20}$)	18.0 ± 1.3a	8.5 ± 0.0a,b	7.3 ± 0.1a,c	8.5 ± 0.2b	5.9 ± 0.6b,c	11.1 ± 1.4a,b,c
Long-chain *n*-alkanes ($\geq C_{20}$)	153.7 ± 12.3a,b	163.6 ± 13.0a,b	192.1 ± 2.2a	169.9 ± 5.0a,b	176.1 ± 1.0b	161.4 ± 10.8a,b
Total *n*-alkanes	171.8 ± 13.6a,b	172.1 ± 13.0a,b	199.4 ± 2.1a	178.3 ± 5.2a,b	182.0 ± 0.4b	172.5 ± 12.2a,b
Short-chain *n*-alkanols ($<C_{20}$)	16.2 ± 0.0a	13.7 ± 0.1b	7.9 ± 0.3c	16.9 ± 0.4a	14.8 ± 0.9a,b	17.3 ± 0.9a,b
Long-chain *n*-alkanols ($\geq C_{20}$)	922.7 ± 44.5a	764.2 ± 32.0c	904.3 ± 0.3b	724.6 ± 5.1a	837.7 ± 31.0a,c	774.7 ± 23.0a,c
Total *n*-alkanols	938.9 ± 44.5a	777.9 ± 31.9a,b	912.2 ± 0.1a	741.5 ± 4.7b	852.5 ± 31.9a,b	792.0 ± 23.9a,b
Short-chain *n*-alkanoic acids ($<C_{20}$)	252.1 ± 12.1b	267.4 ± 10.6b	244.6 ± 3.1b	220.5 ± 12.1b	238.9 ± 21.5a,b	381.3 ± 1.0a
Long-chain *n*-alkanoic acids ($\geq C_{20}$)	179.1 ± 15.8d	292.1 ± 14.3a,b	206.6 ± 12.0c,d	364.7 ± 10.0a	172.3 ± 4.2d	279.1 ± 16.4b,c
Total *n*-alkanoic acids	431.2 ± 27.9d	559.5 ± 3.7c	451.2 ± 15.1d	585.2 ± 2.1b	411.2 ± 25.8d	660.4 ± 15.4a
Short-chain aliphatic lipids[a]	286.3 ± 13.3b	289.5 ± 10.7b	259.8 ± 3.5b	245.9 ± 11.5b	259.6 ± 23.0a,b	409.7 ± 1.3a
Long-chain aliphatic lipids[b]	1255.5 ± 72.6a	1219.9 ± 59.3a	1303.0 ± 9.5a	1259.2 ± 9.8a	1186.2 ± 34.2a	1215.2 ± 50.2a
Fungal-derived steroid[c]	1.5 ± 0.1a,e	1.6 ± 0.0a	0.7 ± 0.0b	2.9 ± 0.0c	2.5 ± 0.0d	1.3 ± 0.0e
Plant-derived steroids[d]	123.7 ± 4.7a,b,d	139.4 ± 2.1a,c,d	114.6 ± 3.8b	153.7 ± 3.5c	138.6 ± 1.8c,d	128.6 ± 6.8a,b,c
Cyclic lipids[e]	151.8 ± 5.7a,b	162.4 ± 2.8a,b	139.4 ± 5.3a	177.8 ± 3.5b,c	177.6 ± 1.5c	153.5 ± 8.3a,b,c

Note : The concentration of a group of solvent extractable organic matter which is significantly different from other crop rotation treatments within the same soil fraction at $P < 0.05$; significant differences between every two treatments are represented by different letters.
[a]Short-chain aliphatic lipids: sum of short-chain ($<C_{20}$) *n*-alkanes, *n*-alkanols and *n*-alkanoic acids.
[b]Long-chain aliphatic lipids: sum of long-chain ($\geq C_{20}$) *n*-alkanes, *n*-alkanols and *n*-alkanoic acids.
[c]Fungal-derived steroid: ergosterol (Otto and Simpson 2005).
[d]Plant-derived steroids: sum of campesterol, stigmasterol, sitosterol and stigmastanol (Otto and Simpson 2005).
[e]Cyclic lipids: sum of cholesterol, ergosterol, campesterol, stigmasterol, sitosterol and stigmastanol.

Table A3. Suberin- and cutin-derived compound concentrations (which were normalized to soil organic carbon (OC) concentration of fractions, μg/g OC) and degradation proxy from different fractions within varied treatments (continuous alfalfa (AAAA), continuous corn (CCCC), corn–corn–alfalfa–alfalfa (CCAA), corn–corn–soybean–soybean (CCSS), corn–corn–soybean–winter wheat (CCSW) and corn–corn–soybean–winter wheat with red clover ($CCSW_{RC}$)) (mean ± standard error; $n = 2$).

	AAAA	CCCC	CCAA	CCSS	CCSW	$CCSW_{RC}$
Light fraction						
ΣS[a]	185.5 ± 2.8	191.3 ± 7.9	123.2 ± 3.9	255.7 ± 9.0	217.0 ± 11.2	183.8 ± 5.7
ΣC[b]	80.1 ± 2.3	46.8 ± 1.5	67.6 ± 0.0	88.0 ± 5.2	65.1 ± 2.0	35.1 ± 2.4
ΣSvC[c]	1472.2 ± 18.9	522.3 ± 32.6	795.2 ± 10.0	744.6 ± 60.6	499.7 ± 26.3	521.3 ± 7.0
ΣSC[d]	1737.8 ± 13.8	760.4 ± 42.1	986.0 ± 6.1	1088.3 ± 56.8	781.8 ± 39.4	740.2 ± 3.7
Suberin/cutin ratio[e]	1.07 ± 0.00	1.25 ± 0.00	1.07 ± 0.01	1.20 ± 0.03	1.27 ± 0.00	1.27 ± 0.02
ω-C_{16}[f]	80.1 ± 2.3	46.8 ± 1.5	67.6 ± 0.0	88.0 ± 5.2	65.1 ± 2.0	35.1 ± 2.4
ΣC_{16}[g]	612.2 ± 3.5	412.3 ± 10.7	529.5 ± 0.9	550.3 ± 1.9	400.5 ± 8.7	355.8 ± 10.6
ω-C_{16}/ΣC_{16}	0.13 ± 0.00	0.11 ± 0.00	0.13 ± 0.00	0.16 ± 0.01	0.16 ± 0.00	0.10 ± 0.00
$F_{53–2000\ \mu m}$ fraction						
ΣS[a]	219.1 ± 23.9	147.5 ± 2.4	186.7 ± 5.6	147.5 ± 13.7	179.5 ± 0.1	163.4 ± 2.5
ΣC[b]	436.2 ± 33.6	137.2 ± 3.0	214.1 ± 10.1	73.0 ± 2.1	66.5 ± 5.1	72.7 ± 6.9
ΣSvC[c]	564.0 ± 57.7	458.9 ± 6.0	634.2 ± 22.7	247.3 ± 17.7	291.0 ± 14.7	273.4 ± 3.4
ΣSC[d]	1219.3 ± 115.1	743.6 ± 0.5	1034.9 ± 27.1	467.8 ± 33.5	537.0 ± 19.9	509.5 ± 6.0
Suberin/cutin ratio[e]	0.78 ± 0.01	1.02 ± 0.00	0.97 ± 0.02	1.23 ± 0.02	1.32 ± 0.03	1.26 ± 0.02
ω-C_{16}[f]	61.2 ± 0.5	53.1 ± 1.8	35.5 ± 0.7	22.7 ± 2.1	23.2 ± 0.7	25.7 ± 1.7
ΣC_{16}[g]	686.8 ± 41.8	384.1 ± 4.6	559.4 ± 13.5	223.7 ± 16.2	257.8 ± 14.2	250.0 ± 1.5
ω-C_{16}/ΣC_{16}	0.09 ± 0.00	0.14 ± 0.00	0.06 ± 0.00	0.10 ± 0.00	0.09 ± 0.00	0.10 ± 0.01
$F_{2–53\ \mu m}$ fraction						
ΣS[a]	165.5 ± 3.7	235.1 ± 12.9	401.4 ± 20.6	211.9 ± 11.0	206.9 ± 1.4	224.1 ± 23.4
ΣC[b]	308.5 ± 11.1	298.1 ± 10.8	167.0 ± 18.8	149.2 ± 0.1	219.3 ± 26.6	220.3 ± 16.5
ΣSvC[c]	448.6 ± 14.1	367.4 ± 2.2	545.5 ± 31.1	276.0 ± 9.5	339.3 ± 7.5	316.9 ± 3.6
ΣSC[d]	922.5 ± 28.9	900.5 ± 4.3	1113.9 ± 70.5	637.2 ± 20.4	765.6 ± 32.7	761.3 ± 3.3
Suberin/cutin ratio[e]	0.81 ± 0.00	0.91 ± 0.03	1.33 ± 0.02	1.15 ± 0.02	0.98 ± 0.05	1.01 ± 0.08
ω-C_{16}[f]	29.2 ± 1.2	42.2 ± 4.7	65.0 ± 0.1	32.7 ± 0.1	36.3 ± 2.6	36.2 ± 1.0
ΣC_{16}[g]	498.2 ± 13.7	586.9 ± 10.1	581.3 ± 41.8	368.6 ± 9.1	492.4 ± 34.4	454.8 ± 21.9
ω-C_{16}/ΣC_{16}	0.06 ± 0.00	0.07 ± 0.01	0.11 ± 0.01	0.09 ± 0.00	0.07 ± 0.00	0.08 ± 0.00
$F_{<2\ \mu m}$ fraction						
ΣS[a]	1737.9 ± 119.9	2693.2 ± 64.1	2515.8 ± 158.8	3564.2 ± 31.3	3205.5 ± 221.0	3051.3 ± 100.3
ΣC[b]	4693.5 ± 468.7	5741.8 ± 321.8	7032.5 ± 654.9	2878.3 ± 367.5	5006.0 ± 453.1	4196.3 ± 370.1
ΣSvC[c]	3216.0 ± 115.2	4232.7 ± 148.3	2525.0 ± 0.8	4383.3 ± 251.3	4534.2 ± 194.3	4132.6 ± 197.6
ΣSC[d]	9647.3 ± 233.7	12 667.6 ± 237.6	12 073.3 ± 495.3	10 825.8 ± 650.1	12 745.6 ± 37.8	11 380.2 ± 467.5
Suberin/cutin ratio[e]	0.63 ± 0.06	0.69 ± 0.02	0.53 ± 0.05	1.10 ± 0.05	0.81 ± 0.07	0.87 ± 0.05
ω-C_{16}[f]	439.3 ± 9.8	544.9 ± 20.4	503.4 ± 31.7	372.4 ± 10.7	679.0 ± 63.9	457.0 ± 27.4
ΣC_{16}[g]	6412.6 ± 276.4	7972.8 ± 144.1	7206.3 ± 537.8	6466.6 ± 520.8	8753.4 ± 305.1	7597.5 ± 533.2
ω-C_{16}/ΣC_{16}	0.07 ± 0.00	0.07 ± 0.00	0.07 ± 0.00	0.06 ± 0.00	0.08 ± 0.01	0.06 ± 0.00

[a] ΣS: sum of suberin-derived compounds (ω-hydroxy acids C_{20}–C_{32}, α,ω-diacids C_{20}–C_{32}, and 9,10-ep C_{18} dioic acid) (Otto and Simpson 2006a).
[b] ΣC: sum of cutin-derived compounds (mid-chain hydroxy C_{14}, C_{15}, C_{17} acids, C_{16} mono- and dihydroxy acids and diacids) (Otto and Simpson 2006a).
[c] ΣSvC: sum of suberin- or cutin-derived compounds (ω-hydroxy acids C_{16}, C_{18}, C_{18} di- and trihydroxy acids 9,10-ep-ω-OH C_{18} acid, and α,ω-diacids C_{16}, C_{18}).
[d] ΣSC: (ΣS+ΣC+ΣSvC) (Otto and Simpson 2006a).
[e] Suberin/cutin ratio: (ΣS+ΣSvC)/(ΣC+ΣSvC) (Otto and Simpson 2006a).
[f] ω-C_{16}: ω-hydroxy C_{16} acid (Otto and Simpson 2006a).
[g] ΣC_{16}: sum of ω-hydroxy C_{16} acid, α,ω-dioic C_{16} acid and C_{16} mid-chain-substituted acids.

Table A4. Lignin-derived phenols (vanillyls (vanillin, acetovanillone and vanillic acid), syringyls (syringaldehyde, acetosyringone and syringic acid) and cinnamyls (*p*-coumaric acid and ferulic acid)) concentrations (which were normalized to soil organic carbon (OC) concentration of fractions, μg/g OC) and degradation proxies from different fractions within varied treatments (continuous alfalfa (AAAA), continuous corn (CCCC), corn–corn–alfalfa–alfalfa (CCAA), corn–corn–soybean–soybean (CCSS), corn–corn–soybean–winter wheat (CCSW) and corn–corn–soybean–winter wheat with red clover ($CCSW_{RC}$)) (mean ± standard error; $n = 2$).

	AAAA	CCCC	CCAA	CCSS	CCSW	$CCSW_{RC}$
Light fraction						
ΣC[a]	2274.3 ± 49.4	5809.2 ± 777.7	5127.9 ± 312.1	4787.4 ± 103.5	5168.9 ± 347.5	5401.7 ± 583.0
ΣS[b]	1729.1 ± 160.3	2701.2 ± 207.2	2489.0 ± 55.5	2965.8 ± 23.0	2359.3 ± 14.4	2651.0 ± 62.5
ΣV[c]	2557.1 ± 50.7	1539.4 ± 84.9	2153.1 ± 27.8	2847.1 ± 81.0	2070.8 ± 6.9	2252.8 ± 94.4
ΣVSC[d]	6560.5 ± 260.4	10 049.8 ± 1069.7	9770.0 ± 395.4	10 600.3 ± 45.4	9599.0 ± 354.9	10 305.6 ± 739.9
ΣS/ΣV	0.68 ± 0.05	1.75 ± 0.04	1.16 ± 0.01	1.04 ± 0.04	1.14 ± 0.01	1.18 ± 0.02
ΣC/ΣV	0.89 ± 0.00	3.76 ± 0.30	2.38 ± 0.11	1.68 ± 0.08	2.50 ± 0.18	2.39 ± 0.16
$(Ad/Al)_v$[e]	0.94 ± 0.09	1.19 ± 0.08	1.09 ± 0.01	1.17 ± 0.00	1.18 ± 0.05	1.08 ± 0.05
$(Ad/Al)_s$[f]	1.10 ± 0.09	1.39 ± 0.05	1.22 ± 0.00	1.20 ± 0.05	1.27 ± 0.05	1.13 ± 0.07
$F_{53–2000\ \mu m}$ fraction						
ΣC[a]	560.6 ± 13.9	1590.9 ± 150.8	926.6 ± 23.9	928.5 ± 44.4	1227.9 ± 25.5	971.4 ± 30.7
ΣS[b]	321.8 ± 3.4	561.7 ± 7.9	398.7 ± 9.6	399.1 ± 13.8	504.1 ± 9.1	447.5 ± 4.6
ΣV[c]	423.4 ± 6.4	404.0 ± 5.3	403.6 ± 9.7	399.1 ± 20.1	459.0 ± 9.6	408.9 ± 9.8
ΣVSC[d]	1305.8 ± 23.7	2556.5 ± 163.9	1728.9 ± 43.2	1726.8 ± 78.3	2191.1 ± 6.7	1827.7 ± 45.1
ΣS/ΣV	0.76 ± 0.00	1.39 ± 0.00	0.99 ± 0.00	1.00 ± 0.02	1.10 ± 0.00	1.09 ± 0.01
ΣC/ΣV	1.32 ± 0.01	3.93 ± 0.32	2.30 ± 0.00	2.33 ± 0.01	2.68 ± 0.11	2.37 ± 0.02
$(Ad/Al)_v$[e]	1.85 ± 0.00	1.78 ± 0.02	1.77 ± 0.08	2.05 ± 0.09	1.77 ± 0.04	1.82 ± 0.01
$(Ad/Al)_s$[f]	1.80 ± 0.13	1.83 ± 0.03	1.86 ± 0.07	2.02 ± 0.04	1.83 ± 0.07	2.11 ± 0.03
$F_{2–53\ \mu m}$ fraction						
ΣC[a]	486.0 ± 49.5	1337.6 ± 89.5	1226.1 ± 73.5	1947.2 ± 108.3	1340.0 ± 10.2	1288.8 ± 16
ΣS[b]	426.6 ± 20.8	769.2 ± 11.6	686.5 ± 16.8	1192.9 ± 5.6	863.2 ± 0.0	815.1 ± 1.9
ΣV[c]	634.0 ± 35.7	838.2 ± 30.5	868.3 ± 16.1	1371.2 ± 3.9	1127.5 ± 7.1	1040.9 ± 18.3
ΣVSC[d]	1546.6 ± 106.0	2945.0 ± 131.6	2780.9 ± 106.4	4511.3 ± 98.9	3330.7 ± 17.3	3144.8 ± 3.6
ΣS/ΣV	0.67 ± 0.01	0.92 ± 0.02	0.79 ± 0.00	0.87 ± 0.00	0.77 ± 0.00	0.78 ± 0.01
ΣC/ΣV	0.76 ± 0.03	1.59 ± 0.05	1.41 ± 0.06	1.42 ± 0.08	1.19 ± 0.00	1.24 ± 0.04
$(Ad/Al)_v$[e]	2.09 ± 0.01	2.31 ± 0.09	2.36 ± 0.10	8.88 ± 0.46	2.28 ± 0.04	2.24 ± 0.19
$(Ad/Al)_s$[f]	1.64 ± 0.11	2.17 ± 0.08	2.16 ± 0.13	8.53 ± 0.04	2.20 ± 0.06	2.23 ± 0.17
$F_{<2\ \mu m}$fraction						
ΣC[a]	476.2 ± 25.4	879.8 ± 50.3	661.2 ± 9.1	506.9 ± 4.1	612.7 ± 6.4	486.0 ± 3.2
ΣS[b]	314.7 ± 13.1	414.6 ± 39.1	405.7 ± 0.7	356.0 ± 9.7	407.1 ± 15.7	283.5 ± 3.8
ΣV[c]	335.0 ± 1.1	334.5 ± 23.1	376.4 ± 0.6	332.0 ± 24.0	365.7 ± 0.5	277.0 ± 3.9
ΣVSC[d]	1125.9 ± 37.4	1628.9 ± 112.5	1443.4 ± 9.2	1194.9 ± 37.8	1385.5 ± 22.5	1046.5 ± 10.9
ΣS/ΣV	0.94 ± 0.04	1.24 ± 0.03	1.08 ± 0.00	1.08 ± 0.05	1.11 ± 0.04	1.02 ± 0.00
ΣC/ΣV	1.42 ± 0.08	2.63 ± 0.03	1.76 ± 0.03	1.53 ± 0.10	1.68 ± 0.02	1.75 ± 0.01
$(Ad/Al)_v$[e]	6.05 ± 0.81	5.09 ± 0.53	4.31 ± 0.14	4.18 ± 0.36	4.03 ± 0.10	3.42 ± 0.19
$(Ad/Al)_s$[f]	3.50 ± 0.10	2.82 ± 0.32	2.22 ± 0.01	1.97 ± 0.02	2.57 ± 0.27	2.92 ± 0.01

[a] ΣC: total cinnamyls (*p*-coumaric acid and ferulic acid) (Otto and Simpson 2006b).
[b] ΣS: total syringyls (syringaldehyde, acetosyringone and syringic acid) (Otto and Simpson 2006b).
[c] ΣV: total vanillyls (vanillin, acetovanillone and vanillic acid) (Otto and Simpson 2006b).
[d] ΣVSC: ΣC + ΣS + ΣV (Otto and Simpson 2006b).
[e] $(Ad/Al)_v$: ratio of vanillic acid to vanillin (Goñi and Hedges 1990a; Otto and Simpson 2006b).
[f] $(Ad/Al)_s$: ratio of syringic acid to syringaldehyde (Goñi and Hedges 1990a; Otto and Simpson 2006b).

Fig. A1. Solid-state ^{13}C NMR spectra of fractionated (light fraction, $F_{53–2000\ \mu m}$, $F_{2–53\ \mu m}$ and $F_{<2\ \mu m}$) soil samples (including continuous alfalfa (AAAA), continuous corn (CCCC), corn–corn–alfalfa–alfalfa (CCAA), corn–corn–soybean–soybean (CCSS), corn–corn–soybean–winter wheat (CCSW) and corn–corn–soybean–winter wheat with red clover ($CCSW_{RC}$)) with four main regions: (*a*) alkyl carbon (0–50 ppm), (*b*) *O*-alkyl carbon (50–110 ppm), (*c*) aromatic and phenolic carbon (110–165 ppm) and (*d*) carboxyl and carbonyl carbon (165–220 ppm) (Baldock et al. 1992; Preston et al. 1997; Simpson et al. 2008).

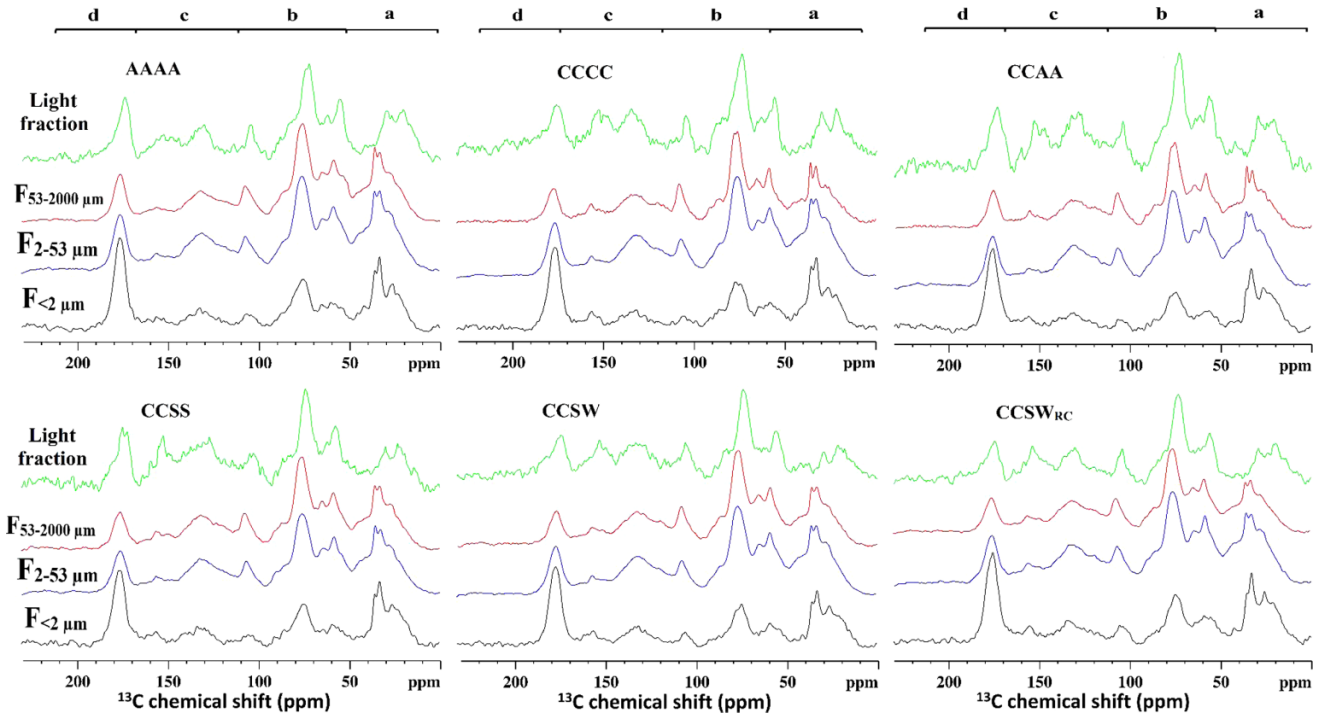

Fig. A2. Linear relations of targeted compound concentrations (μg/g OC of whole soil or fraction) between whole soil and fraction samples and the linear relation between relative soil organic matter (SOM) degradation and carbon to nitrogen (C:N) ratio of light fraction.

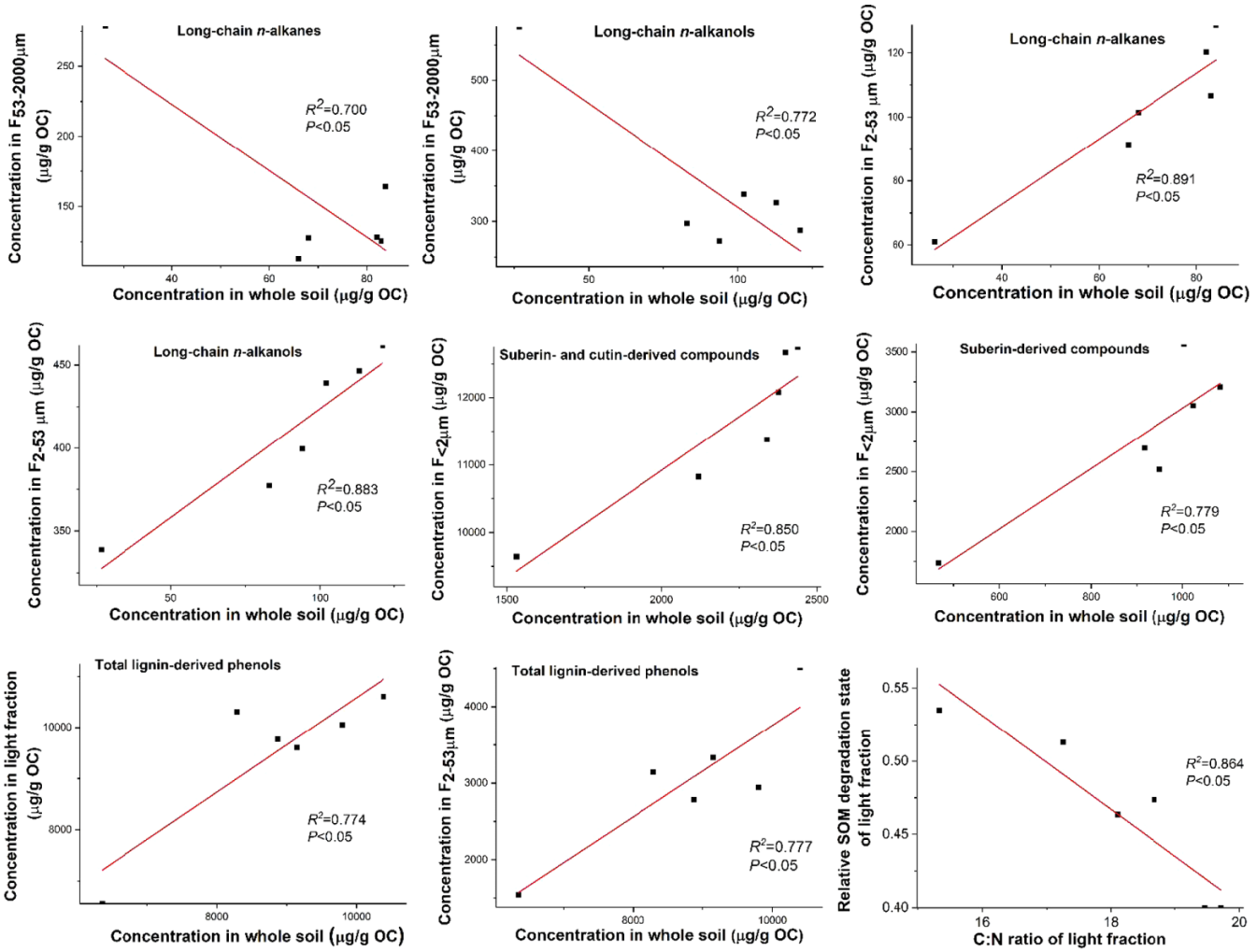

References

Baldock, J.A., Oades, J.M., Waters, A.G., Peng, X., Vassallo, A.M., and Wilson, M.A. 1992. Aspects of the chemical structure of soil organic materials as revealed by solid-state13C NMR spectroscopy. Biogeochemistry **16**: 1–42. doi:10.1007/BF02402261

Goñi, M.A., and Hedges, J.I. 1990a. Potential applications of cutin-derived CuO reaction products for discriminating vascular plant sources in natural environments. Geochim. Cosmochim. Acta **54**: 3073–3081. doi:10.1016/0016-7037(90)90123-3

Goñi, M.A., and Hedges, J.I. 1990b. The diagenetic behavior of cutin acids in buried conifer needles and sediments from a coastal marine environment. Geochim. Cosmochim. Acta **54**: 3083–3093. doi:10.1016/0016-7037(90)90124-4

Hedges, J.I., Blanchette, R.A., Weliky, K., and Devol, A.H. 1988. Effects of fungal degradation on the CuO oxidation products of lignin: A controlled laboratory study. Geochim. Cosmochim. Acta **52**: 2717–2726. doi:10.1016/0016-7037(88)90040-3

Hedges, J.I., and Ertel, J.R. 1982. Characterization of lignin by gas capillary chromatography of cupric oxide oxidation products. Anal. Chem. **54**: 174–178. doi:10.1021/ac00239a007

Kaiser, K., and Benner, R. 2012. Characterization of lignin by gas chromatography and mass spectrometry using a simplified CuO oxidation method. Anal. Chem. **84**: 459–464. doi:10.1021/ac202004r. PMID: 22088192

Otto, A., and Simpson, M.J. 2005. Degradation and preservation of vascular plant-derived biomarkers in grassland and forest soils from Western Canada. Biogeochemistry **74**: 377–409. doi:10.1007/s10533-004-5834-8

Otto, A., and Simpson, M.J. 2006a. Sources and composition of hydrolysable aliphatic lipids and phenols in soils from western Canada. Org. Geochem. **37**: 385–407. doi:10.1016/j.orggeochem.2005.12.011

Otto, A., and Simpson, M.J. 2006b. Evaluation of CuO oxidation parameters for determining the source and stage of lignin degradation in soil. Biogeochemistry **80**: 121–142. doi:10.1007/s10533-006-9014-x

Preston, C.M., Trofymow, J.A., Sayer, B.G., and Niu, J. 1997. 13C nuclear magnetic resonance spectroscopy with cross-polarization and magic-angle spinning investigation of the proximate-analysis fractions used to assess litter quality in decomposition studies. Can. J. Bot. **75**: 1601–1613. doi:10.1139/b97-872

Simpson, M.J., Otto, A., and Feng, X. 2008. Comparison of Solid-State Carbon-13 Nuclear Magnetic Resonance and Organic Matter Biomarkers for Assessing Soil Organic Matter Degradation. Soil Sci. Soc. Am. J. **72**: 268–276. doi:10.2136/sssaj2007.0045